

Modelling a Regional Drought Index in France

Christel PRUDHOMME, CEH Wallingford

Eric SAUQUET, Cemagref Lyon

Hydrological Risks & Resources Section
Risk Analysis and Modelling Group,
CEH Wallingford,
Maclean Building, Benson Lane,
Crowmarsh Gifford,
Wallingford, Oxfordshire, OX10 8BB
Tel. 01491 838800 - Fax 01491 692424

Jan. 2007

Contents

<u>ACKNOWLEDGMENT.....</u>	<u>5</u>
<u>INTRODUCTION.....</u>	<u>7</u>
1 <u>METHODS.....</u>	<u>9</u>
1.1 THE VARIABLES UNDER STUDY.....	9
1.2 REGIONAL CLASSIFICATION BY CLUSTER ANALYSIS.....	10
1.3 DEFINITION OF RDI SPREAD.....	11
1.4 WEATHER TYPE GROUPS.....	12
1.5 MODELLING OF RDI.....	12
1.6 METHOD EVALUATION.....	14
2 <u>DATA15</u>	
2.1 STREAMFLOW DATASET.....	15
2.2 METEOROLOGICAL DATASET.....	18
2.2.1 CIRCULATION AND WEATHER PATTERNS.....	18
2.2.2 RAINFALL AND TEMPERATURE.....	19
3 <u>DERIVING RDI TIME SERIES.....</u>	<u>21</u>
3.1 DEFICIENCY INDEX TIME SERIES.....	21
3.2 RDI CLUSTERS.....	22
3.3 EXPLANATORY ANALYSIS.....	26
4 <u>MODELLING OF RDI AFTER STAHL 2001.....</u>	<u>29</u>
4.1 WEATHER TYPE GROUPS: CP GROUPS.....	29
4.2 RDI MODELLING.....	32
5 <u>A CP CLUSTERING BASED ON RAINFALL OCCURRENCE.....</u>	<u>35</u>
5.1 NEW CP CLUSTERING.....	35
5.2 RDI MODELLING.....	41
5.3 SENSITIVITY ANALYSIS.....	41
6 <u>MODELS EVALUATION.....</u>	<u>45</u>

7	<u>DISCUSSION AND CONCLUSIONS</u>	<u>52</u>
	<u>REFERENCES</u>	<u>54</u>

Acknowledgment

The authors gratefully acknowledge and thank the Euraqua consortium, and in particular CEH and Cemagref Science Programmes, for their financial support.

Introduction

The project was set up to build the capacity and research skills of CEH Wallingford and Cemagref Lyon in the seasonal forecasting of river flow extremes, and in particular of droughts.

The forecasted rise in global temperature in the future by Global Climate Models (IPCC, 2001), the extent and dramatic consequences of recent drought such as that of 2003 in France and Europe or the long river flow deficit of 2005/2006 in Southern Britain could be precursor signs that some difficult challenges may be facing water managers in the future decades. Anticipating large droughts (in terms of severity of the deficit, duration of drought, or spatial extent of regions affected) would help efficient planning strategy and management, avoiding resorting to measures such as house pipe bans or limited abstraction.

In 2001, the European project ARIDE (ENV4-CT97-0553) provided an assessment of the regional impact of droughts in Europe (Demuth and Stalh, 2001). Within the project, a methodology for the seasonal forecasting of a Regional Streamflow Deficiency Index was developed and tested on most Western Europe regions. However, due to the lack of long-record river flow data available for the project, the method was not applied on in France.

The aim of this collaborative project was to test the methodology developed within ARIDE in France, and investigate alternative forecasting routes. All models were tested on the most recent droughts including that of 2003, not part of the ARIDE data set.

1 Methods

Drought definitions are numerous but generally refer to a period in time when there is a decrease in the water availability compared to a ‘normal’ period. Drought definitions are therefore relative, and hydrological drought can be defined in many ways, including climatological, agro-meteorological, relative to streamflow, groundwater or operational use (Tate and Gustard, 2000).

As basis of this study, the drought definition of the ARIDE project (Demuth and Stahl, 2001) and Stahl (2001) was taken, where the concept of threshold-level is used to define a drought. The event definition considers periods of streamflow deficiency as a departure or ‘anomaly’ from the ‘normal’ annual low-flow cycle, the normality being established according to a varying threshold. This varying threshold is designed for seasonality in streamflow to be accounted for, i.e. regular (and expected) summer low flow periods are only part of a drought if the flow is lower than the usual flow of the season, rather than compared to an annual threshold such as a proportion of the module. Because the threshold is calculated at a point, it also includes regional streamflow specificity (e.g. in Alpine regions, winter low flows are expected as water precipitates and is stored as snow rather than producing runoff).

This definition of drought relies on two indicators, the Deficiency Index DI , that characterises a period of the record at a given location with water availability lower than usual (i.e. deficiency for that station); and a Regional Deficiency Index RDI , that characterises the extent of this deficit in availability within a geographical region. If the deficit is generalised across the region, then the period considered is defined as a drought.

1.1 The variables under study

The variables under study are an at-site daily deficiency indicator DI and a Regional streamflow Deficiency Index (RDI), characterising the extent of the deficiency at large spatial scale. Both indices are free from seasonal effect, as they are based on a varying threshold.

Let us consider one of the gauging stations with N years of record. The at-site index for each day J of the year is calculated as follows:

- select the flow Q recorded within the time window $[J-D ; J+D]$ for the N years of record;
- order all the selected values to form a Flow Duration Curve specific to the J^{th} day of the year;

- derive the threshold $Q_{90}(J)$, the value of streamflow equalled or exceeded 90% of the time;
- define a new time series $DI(t)$, for all the days in the series of day J:

$$\begin{aligned} \text{Equation 1} \quad DI(t) &= 1 && \text{if } Q(t) \leq Q_{90}(J) \\ DI(t) &= 0 && \text{if } Q(t) > Q_{90}(J) \end{aligned}$$

Note that, by definition, exactly, 90% of the time series DI are 0.

The use of a time window of $2D+1$ length $[J-D; J+D]$ for the construction of a smooth daily flow duration curve is necessary as record length is limited, and samples uniquely based on the N values of $Q(J)$ would be too small.

Consider now a region and the dataset of M gauging stations located within this region. The Regional Deficiency Index RDI is the spatial mean of DI , interpreted as the proportion of basins affected by deficiency:

$$\text{Equation 2} \quad RDI(t) = \frac{1}{M} \sum_{i=1}^M DI_i(t)$$

Stahl (2001) recommends a value of $RDI = 0.3$ as a minimum to define the existence of a severe drought (30% of the region).

1.2 Regional classification by cluster analysis

Drought events are phenomena with variable scales, both in time and space. One common way to explore this variability and to understand underlying processes at large scale is to perform regional analysis. The objective is here to delineate homogenous region in a sense that rivers within the same in group are expected to be affected by deficit ($DI=1$) or not ($DI=0$) at the same time. Different methods to form groups exist. Cluster analysis is one of the most common approaches. It is an exploratory statistical tool designed to objectively form homogeneous groups of individuals or objects. The computation of clusters requires sets of rules such as the final number of groups, the algorithm, the criterion of dissimilarity and homogeneity. These rules may influence the final classification. The method used by Stahl (2001) is based on the following rules:

- the selected distance measure between two objects is the Binary Euclidean distance:

$$\text{Equation 3} \quad dist(i, j) = \sqrt{\sum_t (1 - \delta(DI_i(t) - DI_j(t)))} \text{ where } \delta(x) = \begin{cases} 1 & \text{if } x = 0 \\ 0 & \text{if } x \neq 0 \end{cases}$$

This distance was considered as it unites catchments with similar response to meteorological dry periods.

- The clustering algorithm relies on the Ward's method. Cluster membership is assessed by computing, for each object of a candidate cluster, the total sum of squared deviations from the mean of the cluster. The criterion for fusion is that it should produce the smallest possible increase in the sum of squares error.
- The optimal number of groups is fixed considering:
 - o the agglomeration schedule, which quantifies the increase in distance between clusters from one stage to another. A noticeable jump in the distance from one clustering solution to the next one indicates that two non-homogeneous groups have been combined and the grouping should therefore be stopped at the previous grouping level;
 - o the deviation of our variable of interest, RDI , computed for each group according to *Equation 4*, to the expected RDI_{theo} if all stations of the group behave exactly in the same way. By definition of DI , 90% (respectively 10%) of the RDI time series should be equal to 0 (respectively 1). An index quantifying this deviation is derived from the observed cumulative distribution function.

The final clusters comprise a set of stations (or regions) all expected to respond similarly to drought conditions (concomitant streamflow deficiency).

1.3 Definition of RDI spread

River streamflow being a measure of a physical phenomenon continuous in time, there is a strong autocorrelation of river flow series, stronger when the considered flow represents an average over a short time period. For daily flows, 1-day autocorrelation is significant. When analysing potential relationship between river flow and other physical phenomenon, such as atmospheric circulation pattern, this existing autocorrelation in river discharge could lead to statistical links that are artefact of this autocorrelation rather than resulting from real physical phenomenon. To avoid this problem and to account for persistency of drought conditions Stahl (2001) removed the autocorrelation in analysing an intermediary variable, derived from the regional streamflow deficiency index RDI by Equation 5:

$$\text{Equation 5} \quad y(t) = RDI(t) - RDI(t-1)$$

$y(t)$ represents the spread (when positive) or shrinkage (when negative) of the drought extent of a region, as defined by $RDI(t)$. Stahl (2001) found significant frequency anomalies associated with some weather types during severe drought deficiency periods compared to their average frequency of occurrence. The evolution of the drought extent was shown to be associated with dry/wet periods, and therefore could be linked to particular weather types The

model suggested by Stahl (2001) makes use of this assumption, linking the day-to-day evolution of a severe regional streamflow deficiency with the occurring weather type (or anomaly).

1.4 Weather type groups

Weather type classifications usually produce a large number of different conditions (e.g. Grosswetterlagen classification has 29 weather types, the Lamb classification for the British isles has 28 categories), some of these categories only occurring few days in the year. To avoid building models with too many degrees of freedom (29 coefficients) or including links to events rarely observed, Stahl (2001) recommended to group weather types according to their effect on the *RDI*. For each region, the frequency of occurrence of a given weather type during period of severe drought (defined as $RDI > 0.3$) was compared to the frequency of occurrence of the same weather type during the whole period 1965-2000. The weather types showing similar frequency anomalies were regrouped in Circulation Pattern groups (CP groups) following Table 1-1.

CP group name	Frequency anomaly
CPg1	> 10%
CPg2	5% to 10%
CPg3	2% to 5%
CPg4	0.5% to 2%
CPg5	-0.5% to 0.5%
CPg6	-2% to -0.5%
CPg7	-5% to -2%
CPg8	-10% to -5%
CPg9	< -10%

Table 1-1: Basis of weather types groupings (CP groups, after Stahl, 2001)

To account for seasonal variation in the occurrence of the weather types, seasonal groupings are recommended, with seasons defined as winter (December to February), spring (March to May), summer (June to August), and autumn (September to November).

1.5 Modelling of RDI

Following Stahl (2001), *RDI* is modelled in two stages, using a basic recursive process, for each of the given regions.

First, the modelling of the change in the drought extent $y(t)$ is given by Equation 6

$$\text{Equation 6} \quad y(t) = y(t-1) + \sum_{i=1}^n b_i Z_i$$

with n , the number of CP groups. The occurrence of a weather type within a CP group i is given by Z_i (equal to 1 if one weather type of the group occurred, 0 if not). $y(t)$ represents the change of the streamflow deficit extent in the region (i.e. is it spreading or shrinking). $y(t)$ is bound: when the entire region is already affected by severe droughts (all stations have a DI equal to 1), no further spread would be possible if another ‘dry’ weather type were to occur. The values for the upper and lower boundaries are defined arbitrarily as:

$$\begin{aligned} \text{Equation 7} \quad y(t) &= 1 && \text{if } y(t) > 1 \\ y(t) &= -1 && \text{if } y(t) < -1 \end{aligned}$$

Second, $RDI(t)$ is derived from $y(t)$. By definition, the mean of RDI is 0.1, as RDI is non-nil only when the flow exceeds Q90, i.e. by definition 10% of the time. To obtain a simulated RDI , only the part describing the streamflow deficiency spread has to be selected from the $y(t)$ series. This is achieved by finding the threshold y_0 so that the transformed series RDI_{sim} has a mean value equal to 0.1 (Equation 8):

$$\begin{aligned} \text{Equation 8} \quad RDI_{sim}(t) &= \frac{y(t) - y_0}{1 - y_0} && \text{if } y(t) > y_0 \\ RDI_{sim}(t) &= 0 && \text{if } y(t) < y_0 \end{aligned}$$

A sequential algorithm testing a number of parameter set combinations was used to determine the parameter set associated with the largest goodness-of-fit for RDI . Because there is no analytic solution for Equation 8, it was solved by an iterative procedure. For each parameter set, y_0 was optimised (using the dichotomy method) so that the average of RDI_{sim} was as close as possible from 0.1 (definition).

The goodness-of-fit based on the Pearson product moment coefficient (Equation 9) was recommended as objective function by Stahl (2001):

$$\text{Equation 9} \quad r_{pearson} = \frac{m \sum_{t=1}^m x_t y_t - \sum_{t=1}^m x_t \sum_{t=1}^m y_t}{\sqrt{m \sum_{t=1}^m x_t^2 - \left(\sum_{t=1}^m x_t \right)^2} \sqrt{m \sum_{t=1}^m y_t^2 - \left(\sum_{t=1}^m y_t \right)^2}}$$

with x : RDI_{sim} and y : RDI_{obs} for each day t of the m days of the calibration series

A second, independent, measure of goodness-of-fit is the agreement index. The index varies between 0 (no agreement) to 1 (full agreement), taking into account the differences between the observed and the simulated values (Equation 10).

$$\text{Equation 10} \quad a = 1.0 - \frac{\sum_{t=1}^m (RDI_{obs_t} - RDI_{sim_t})^2}{\sum_{t=1}^m \left(\left| RDI_{sim_t} - \overline{RDI_{obs}} \right| + \left| RDI_{obs_t} - \overline{RDI_{obs}} \right| \right)^2}$$

1.6 Method evaluation

The method as defined by Stahl (2001) and used in Europe was tested on a selected number of regions in France (excluded from the original ARIDE study). The calibration of the models was undertaken on the 1965-2000 period. The models were then evaluated on the independent period 2001-2004, that includes the 2003 drought. An alternative technique for the weather type grouping was also evaluated on the same series to assess potential improvements for the modelling (and potential forecasting) of drought in France.

2 Data

2.1 Streamflow dataset

The French hydrological database HYDRO supplies time series of observed and naturalised discharges. For this study, the reference period was set to 1965-2004, including the most recent drought of 2003. The total data set consists of 121 gauged catchments with limited artificial impact, with minimal gaps in the data record and with high quality data (Table 2-1, Figure 2-1a). The drainage area of the catchments ranges from 5 to 109 930 km². The highest density of stations is in the Central Massif (central France). Most of the selected catchments exhibit rainfall fed flow regime with low flows in summer and high flows in winter.

Code	Station	Easting km	Northing km	Area km ²	Mean monthly discharge (m ³ /s)											
					JAN	FEB	MAR	APR	MAY	JUN	JUL	AUG	SEP	OCT	NOV	DEC
A3472010	LA ZORN A WALTENHEIM-SUR-ZORN	989.42	2429.91	688	9.42	11.07	9.04	7.12	6.12	4.50	3.39	2.93	2.98	3.98	5.40	8.90
A4200630	LA MOSELLE A ST-NABORD	918.43	2349.43	621	40.20	38.21	34.42	28.69	19.55	14.14	10.62	8.02	10.87	19.83	31.16	41.88
A4250640	LA MOSELLE A EPINAL	906.14	2359.87	1220	61.83	59.76	53.59	45.76	35.95	25.84	19.20	13.92	16.86	29.81	44.99	62.84
A5431010	LE MADON A PULLIGNY	880.25	2400.79	940	21.27	20.89	15.43	11.66	7.53	5.05	3.20	2.53	2.93	5.81	10.68	20.50
A5730610	LA MOSELLE A TOUL	862.63	2413.64	3350	112.44	111.84	93.47	77.10	53.60	37.02	25.16	18.71	23.26	42.92	70.30	108.57
A6941020	LA MEURTHE A MALZEVILLE (2)	882.88	2418.86	2960	65.64	70.08	58.49	48.19	38.61	29.05	19.28	15.24	16.74	25.18	38.36	64.84
D0137010	L' HELPE MINEURE A ETROEUNGT	714.1	2564	175	3.65	3.15	2.83	2.01	1.20	1.22	1.09	0.72	0.73	1.18	1.99	3.17
D0156510	L' HELPE MAJEURE A LIESSIES	724.8	2570.5	198	4.41	4.24	3.33	2.53	1.44	1.12	0.97	0.63	0.83	1.43	2.48	4.36
E1727510	L' ECAILLON A THIANT	679.5	2590.5	173	1.53	1.59	1.64	1.50	1.27	1.13	1.03	0.93	0.90	0.95	1.18	1.47
E1766010	LA RHONELLE A AULNOY-LEZ-VALENCIENNES	685.2	2593.5	88.4	0.90	0.92	0.93	0.80	0.64	0.51	0.44	0.38	0.38	0.41	0.55	0.82
E3511220	LA LYS A DELETTES	591.4	2624.8	158	3.19	3.17	2.82	2.47	2.05	1.66	1.37	1.14	1.08	1.31	1.88	2.68
E4035710	L' AA A WIZERNES	593.5	2634.9	392	7.32	7.75	7.33	6.66	5.65	4.57	3.81	3.16	2.95	3.23	4.34	5.89
E5400310	LA CANCHE A BRIMEUX	564	2606	894	14.04	14.71	14.63	14.25	13.26	12.00	10.83	9.65	9.32	9.68	10.98	12.55
E5505720	L' AUTHIE A DOMPIERRE-SUR-AUTHIE	570.1	2590	784	8.44	9.13	9.52	9.61	9.10	8.35	7.69	6.94	6.56	6.47	6.78	7.52
E6470910	LA SOMME A EPAGNE-EPAGNETTE	563.7	2567	5560	40.82	43.82	43.40	42.15	39.30	35.01	30.91	27.48	27.01	28.80	32.03	36.30
H0400010	LA SEINE A BAR-SUR-SEINE	751.98	2348.38	2340	47.86	51.44	38.02	32.21	24.21	14.54	9.57	6.49	7.91	13.28	21.39	40.22
H1501010	L' AUBE A ARCIS-SUR-AUBE	733.35	2394.8	3590	59.08	65.63	53.65	45.83	33.20	21.98	18.03	14.31	14.91	19.74	27.97	49.66
H2342010	LE SEREIN A CHABLIS	709.62	2314.17	1120	16.78	18.66	12.58	10.98	7.30	4.28	2.12	1.11	1.52	3.60	6.76	14.37
H5071010	LA MARNE A ST-DIZIER	791.09	2407.88	2380	46.81	47.78	34.00	30.51	20.50	14.67	11.55	8.09	10.52	17.47	29.12	48.51
H5172010	LE SAULX A VITRY-EN-PERTHOIS	768.284	2418.924	2100	53.12	53.09	40.50	32.24	19.80	12.22	10.06	7.23	7.45	13.66	25.01	47.46
H6201010	L' AISNE A MOURON	777.92	2481.43	2280	49.98	53.42	41.62	33.21	19.33	12.39	10.47	6.98	6.22	12.89	22.01	44.71
H7401010	L' OISE A SEMPIGNY	647.6	2507.2	4290	56.77	60.64	53.72	48.30	34.43	24.44	20.36	15.12	14.40	19.80	28.88	47.32
I9221010	LA SELUNE A DUCEY	336.7	2404.9	720	21.04	21.34	16.73	12.53	9.34	6.52	4.48	3.33	3.71	6.34	11.03	16.75
J0621610	LA RANCE A GUENROC	274.1	2377.7	380	6.15	6.10	4.42	3.11	2.62	1.07	0.62	0.35	0.43	1.26	2.40	4.44
K0433010	LE LIGNON VELLAVE A YSSINGEAUX	745.599	2019.581	350	8.17	8.68	8.73	9.58	8.77	4.43	2.12	1.26	3.16	6.62	8.12	8.50
K0454010	LA DUNIERES A STE-SIGOLENE	747.11	2025.91	228	4.24	4.41	4.36	4.78	4.72	2.81	1.52	1.05	1.55	2.90	3.60	4.05

Table 2-1: Dataset of French gauging stations

Code	Station	Easting km	Northing km	Area km²	Mean monthly discharge (m³/s)											
					JAN	FEB	MAR	APR	MAY	JUN	JUL	AUG	SEP	OCT	NOV	DEC
K0523010	L' ANCE DU NORD A ST-JULIEN-D'ANCE	725.698	2035.389	354	6.49	6.86	6.62	6.59	6.09	3.53	1.80	1.35	1.54	2.87	4.26	6.10
K0550010	LA LOIRE A BAS-EN-BASSET	739.61	2034.33	3234	50.27	51.53	50.03	51.99	51.86	27.88	14.85	11.30	15.71	32.63	42.18	49.51
K0673310	LA COISE A ST-MEDARD-EN-FOREZ	759.05	2069.57	181	2.51	2.41	2.09	2.05	2.22	1.25	0.58	0.46	0.73	1.27	1.90	2.39
K0910010	LA LOIRE A VILLEREST	732.25	2112.78	6585	97.12	101.15	91.04	91.91	91.58	49.56	25.56	23.74	38.74	55.09	80.10	85.44
K1391810	L' ARROUX AU VERDIER	726.69	2167.69	3166	73.86	78.70	51.25	42.47	32.89	17.17	8.60	7.25	9.86	20.30	37.75	64.15
K1503010	LA BESBRE A CHATEL-MONTAGNE	703.9	2126.1	135	3.94	4.29	3.38	3.45	3.30	2.17	1.18	0.84	1.28	1.85	2.79	3.92
K2330810	L' ALLIER A VIEILLE-BRIOUDE	683.96	2029.67	2269	39.57	41.13	40.44	44.43	41.39	21.42	11.73	10.60	13.14	24.33	33.47	38.76
K2363010	LA SENOUIRE A PAULHAGUET	693.21	2022.7	155	2.28	2.34	2.20	2.35	2.46	1.41	0.58	0.39	0.53	1.03	1.51	2.10
K2514010	L' ALLANCHE A JOURSAC	650.98	2015.52	157	4.64	5.11	4.54	4.30	3.37	1.89	1.13	0.88	1.14	1.80	2.65	4.17
K2523010	L' ALAGNON A NEUSSARGUES-MOISSAC	652.5	2015.5	310	9.63	10.25	9.36	9.77	7.96	4.11	2.38	1.82	2.66	4.74	6.92	10.01
K2654010	LA COUZE D'ISSOIRE A ST-FLORET	660.14	2061.41	216	7.34	7.63	6.60	6.67	5.35	3.31	1.94	1.45	1.79	2.94	4.61	7.04
K2674010	LA COUZE DE CHAMPEIX A MONTAIGUT-LE-BLANC	658.94	2065.69	159	4.01	4.01	3.38	3.52	3.24	1.97	1.14	0.96	1.23	1.93	2.76	3.91
K2871910	LA DORE A TOURS-SUR-MEYMONT	697.98	2077.88	800	15.84	16.92	16.40	16.71	15.99	9.57	4.53	3.58	4.15	6.27	9.97	14.66
K2884010	LA FAYE A AUGEROLLES	698.25	2078.65	72	2.26	2.39	2.21	2.29	2.14	1.54	0.89	0.76	0.88	1.11	1.58	2.12
K3222010	LA SIOULE A PONTGIBAUD	639.38	2092.79	353	10.11	10.06	8.17	8.26	7.00	5.04	3.17	2.50	3.04	4.03	6.38	9.27
K3292020	LA SIOULE A ST-PRIEST-DES-CHAMPS	635.55	2108.24	1300	29.96	30.90	23.86	23.47	21.94	14.06	7.07	5.69	7.54	11.18	17.27	26.64
K4470010	LA LOIRE A BLOIS	524.68	2287.91	38320	599.11	679.39	550.65	497.55	500.82	293.8	160.6	119.4	137.9	196.8	303.2	500.99
K5090910	LE CHER A CHAMBOCHARD	616.28	2130.51	517	11.07	12.44	8.17	7.68	7.83	4.73	1.98	1.28	2.43	3.59	5.18	9.08
K5183010	LA TARDES A EVAUX-LES-BAINS	607.49	2131.65	854	16.85	17.89	12.64	11.57	9.95	5.81	2.41	1.62	2.42	3.96	7.41	13.93
K5200910	LE CHER A TEILLET-ARGENTY	615.5	2138.05	1600	29.64	32.38	21.74	20.63	19.42	11.19	4.66	3.33	5.38	8.43	14.04	25.33
L0140610	LA VIENNE A ST-PRIEST-TAURION	527.26	2098.65	1156	40.89	42.30	33.27	31.07	25.78	18.83	12.74	10.90	13.72	17.56	23.97	36.29
L0231510	LE TAURION A PONTARION	561.81	2110.52	388	11.82	12.15	9.28	8.86	7.51	4.79	3.05	2.10	2.57	3.97	6.20	9.63
L0400610	LA VIENNE AU PALAIS-SUR-VIENNE	521.49	2096.51	2296	78.68	81.51	64.50	60.58	50.32	34.59	22.67	18.70	21.72	28.79	41.01	64.91
L3200610	LA VIENNE A INGRANDES	464.24	2210.48	10050	215.00	220.95	166.42	151.79	121.68	78.47	48.60	38.03	45.33	64.27	105.2	172.50
L4010710	LA CREUSE A FELLETIN	587.1	2097.9	165	6.52	6.67	5.18	5.18	4.16	2.76	1.60	1.12	1.49	2.02	3.41	5.63
L4033010	LA ROZEILLE A MOUTIER-ROZEILLE	591.66	2102.16	186	4.77	4.88	3.78	3.69	3.34	2.13	0.96	0.63	0.82	1.29	2.16	3.66
L4220710	LA GRANDE CREUSE A FRESSELINES	549.23	2153.2	1235	29.41	32.08	23.85	22.39	19.26	11.26	5.60	3.44	4.74	7.42	13.28	24.16
L4411710	LA PETITE CREUSE A FRESSELINES	549.8	2154.02	850	16.90	18.64	13.09	11.13	9.15	4.65	2.64	1.92	2.51	3.96	7.22	13.89
L4530710	LA CREUSE A EGUZON-CHANTOME	544.4	2161.9	2400	52.60	57.87	42.51	38.77	32.18	17.59	9.16	6.37	8.57	13.30	23.59	43.62
L8000020	LA LOIRE A SAUMUR	418.56	2253.15	81200	1225.5	1325.9	1078.1	923.36	856.23	520.0	301.3	221.4	257.2	369.7	592.0	954.82
M0500610	LA SARTHE A SPAY	436.23	2326.07	5285	73.18	71.39	57.79	43.57	31.50	20.05	14.50	11.51	12.62	19.46	31.99	52.49
M5300010	LA LOIRE A MONTJEAN-SUR-LOIRE	358.7	2270.92	109930	1614.1	1773.6	1400.7	1163.2	1014.7	624.0	362.7	255.5	301.3	461.4	755.9	1220.7
O0105110	LA NESTE DE CAP DE LONG A ARAGNOUET	417.73	1758.64	5	0.03	0.02	0.02	0.04	0.26	0.84	0.82	0.41	0.23	0.17	0.10	0.04
O0126210	LA NESTE DE RIOUMAJOU A TRAMEZAYGUES	433.19	1755.63	63.7	0.92	0.81	1.10	2.07	4.99	5.90	2.91	1.44	1.35	1.86	1.84	1.11
O0362510	LE SALAT A SOUEIX (KERCABANAC)	508.21	1766.91	379	12.82	13.53	16.35	24.63	34.97	28.12	14.49	9.01	8.95	10.50	12.77	13.64
O0592510	LE SALAT A ROQUEFORT-SUR-GARONNE	488.6	1796.04	1570	43.71	48.54	50.21	66.63	81.05	59.09	30.99	20.15	20.57	26.24	33.62	45.18
O1115010	L' ARTIGUE A AUZAT	524.64	1745.52	23.8	0.38	0.38	0.65	1.25	3.10	3.92	2.11	1.04	0.78	0.88	0.72	0.52
O3011010	LE TARN AU PONT-DE-MONTVERT	713.42	1929.87	67	4.73	3.76	4.16	5.73	4.82	1.93	0.78	0.38	1.60	4.93	6.07	4.74
O3141010	LE TARN A ST-PIERRE DES TRIPIERS	670.17	1911.55	925	45.39	43.62	35.96	38.50	33.82	17.93	10.19	8.09	13.97	31.47	40.01	41.79
O4102510	L' AGOUT A FRAISSE-SUR-AGOUT	637.46	1845.09	48	2.55	2.56	2.33	2.05	1.63	0.80	0.35	0.18	0.33	1.52	2.06	2.60
O5292510	L' AVEYRON A LAGUEPIE	570.77	1905.86	1540	34.50	40.14	27.25	24.80	23.04	10.66	4.70	3.28	4.55	9.62	16.55	31.40
O5344010	LE VIOULOU A TREBON	637.5	1912.64	57	2.07	2.23	1.59	1.41	1.15	0.54	0.23	0.10	0.16	0.63	1.10	1.81
O5572910	LE VIAUR A LAGUEPIE	570.47	1904.66	1530	27.36	32.57	23.40	21.61	19.58	9.89	4.87	3.21	3.88	6.66	12.43	25.25
O5882510	L' AVEYRON A PIQUECOS	520.21	1899.27	5170	92.17	110.83	76.11	69.07	62.61	29.43	12.64	7.86	11.95	22.49	41.59	84.63
O7054010	LA COLAGNE A ST-AMANS	685.48	1961.78	89	1.98	2.25	2.29	2.64	2.17	1.15	0.53	0.40	0.52	1.10	1.61	2.12
O7101510	LE LOT A BANASSAC	668.24	1937.88	1160	23.80	25.32	21.14	23.30	20.12	10.54	4.75	3.25	4.89	11.82	18.51	23.40
O7131510	LE LOT A LASSOUTS (CASTELNAU)	642.03	1944.6	1650	39.03	42.20	33.99	35.29	29.66	15.45	7.47	5.22	7.46	17.95	27.96	38.48
O7272510	LA TRUYERE AU MALZIEU-VILLE	680	1982.1	542	11.51	12.53	11.12	11.80	10.93	6.22	3.04	2.39	2.83	5.73	8.13	10.92
O7354010	LA LANDER A ST-GEORGES	662.5	2001.6	310	6.54	6.48	5.27	4.99	4.02	1.77	0.77	0.58	1.17	2.40	3.75	6.01

Table 2-1 (cont.)

Code	Station	Easting km	Northing km	Area km²	Mean monthly discharge (m³/s)											
					JAN	FEB	MAR	APR	MAY	JUN	JUL	AUG	SEP	OCT	NOV	DEC
O7444010	LE BES A ST-JUERY	659.3	1980.9	283	12.25	13.29	11.83	12.69	8.42	4.22	1.99	1.54	2.53	6.33	9.34	12.62
O7502510	LA TRUYERE A NEUVEGLISE	658.2	1991.7	1782	41.10	43.59	37.83	38.26	31.56	16.83	7.37	5.76	8.89	19.24	27.94	39.52
O7592510	LA TRUYERE A STE-GENEVIEVE-SUR-ARGENCE	631.2	1981.2	2462	64.67	70.37	58.96	58.48	46.47	25.39	11.86	8.42	13.89	29.68	44.81	64.00
O7635010	LA BROMME A BROMMAT (EDF)	627.2	1981.3	111	6.00	6.05	4.98	4.67	3.44	1.94	1.06	0.63	1.46	2.78	4.42	5.78
O8231510	LE LOT A CAHORS	529.1	1939.1	9170	236.05	270.74	197.73	186.44	166.10	98.42	53.71	31.78	56.46	104.7	157.2	231.03
P0010010	LA DORDOGNE A ST-SAUVES-D'AUVERGNE	624.97	2068.01	87	4.87	4.93	4.70	5.49	4.70	3.26	2.19	1.74	2.20	3.04	4.04	4.80
P0115010	LA BURANDE A LA TOUR-D'AUVERGNE	628.18	2058.88	20.4	1.21	1.23	1.22	1.34	1.07	0.79	0.60	0.49	0.65	0.92	1.17	1.33
P0115020	LA BURANDE A SINGLES	616.1	2060.4	80	4.20	4.33	4.03	4.12	3.09	2.08	1.26	0.95	1.46	2.49	3.59	4.48
P0190010	LA DORDOGNE A BORT-LES-ORGUES	612.8	2045.8	1010	38.04	38.39	30.90	30.56	25.64	17.04	9.39	7.37	10.70	17.54	26.60	35.36
P0364010	LA SANTOIRE A CONDAT	632.6	2036.999	172	7.07	7.09	6.30	6.59	5.19	2.65	1.44	0.97	1.90	3.68	5.24	7.14
P0885010	LE MARS A BASSIGNAC	603.5	2032.5	117	5.65	6.09	5.08	5.19	4.21	2.27	1.15	0.91	1.72	3.18	4.86	6.16
P0894010	LA SUMENE A BASSIGNAC	603.8	2033.3	401	11.61	12.01	9.53	9.66	7.79	4.41	2.41	1.99	3.64	6.45	9.74	12.22
P1114010	LA LUZEGE A MAUSSAC	585.5	2052.1	84.9	3.71	3.55	2.65	2.48	1.91	1.25	0.77	0.52	0.83	1.45	2.28	3.33
P1422510	LA MARONNE A STE-EULALIE	602.88	2012.73	112	6.18	6.63	5.34	5.80	4.50	2.76	1.50	1.21	2.13	3.88	5.06	6.53
P1502510	LA MARONNE A PLEAUX	588.8	2009.2	513	23.55	25.03	19.49	18.70	15.50	8.61	4.10	2.70	5.73	11.34	17.57	22.97
P3021010	LA VEZERE A BUGEAT	567.8	2067.2	143	7.63	7.44	5.53	5.15	3.91	2.67	1.75	1.24	1.92	3.33	5.16	7.18
P3922510	LA CORREZE A BRIVE-LA-GAILLARDE	533.16	2018.03	947	35.67	37.14	28.07	27.33	22.44	14.02	9.00	5.80	7.61	12.85	20.69	30.95
P4161010	LA VEZERE A MONTIGNAC	507.402	2007.887	3125	96.85	103.60	78.60	73.91	61.07	40.99	26.51	17.57	23.15	37.39	58.32	88.36
Q5501010	LE GAVE DE PAU A BERENX	341.91	1838.49	2575	97.98	100.40	89.68	107.52	131.49	117.4	73.61	46.48	42.44	60.96	79.11	102.08
Q6142910	LE GAVE D'OSSAU A OLORON-STE-MARIE	362.67	1799.48	488	19.66	20.31	20.17	28.22	40.89	31.19	15.04	7.20	8.28	14.90	19.73	22.19
Q7002910	LE GAVE D'OLORON A OLORON-STE-MARIE	359.67	1803.6	1085	57.05	58.36	57.54	79.09	98.70	67.55	35.00	20.88	23.98	40.17	54.42	62.93
Q7412910	LE GAVE D'OLORON A ESCOS	330.27	1832.32	2456	127.42	130.57	119.91	153.51	167.93	107.6	55.04	35.19	41.13	74.50	106.6	136.28
U0230010	LA SAONE A CENDRECOURT	868.91	2323.73	1130	31.25	31.44	24.27	19.93	14.40	9.48	6.78	5.26	6.60	11.36	18.35	29.75
U0610010	LA SAONE A RAY-SUR-SAONE	862.45	2292.14	3740	109.41	107.05	83.44	66.34	50.22	31.28	21.98	17.18	22.04	41.24	67.08	104.14
U2122010	LE DOUBS A GOUMOIS	948.89	2262.66	1060	36.96	39.87	41.42	41.70	29.64	23.63	17.21	13.99	17.83	23.91	31.93	39.48
U2142010	LE DOUBS A GLERE (COURCLAVON)	954.13	2271.056	1240	43.29	46.46	48.16	47.88	34.51	27.59	19.39	15.66	19.88	27.27	36.78	46.25
U4710010	LA SAONE A COUZON-AU-MONT-D'OR (1)	794.05	2097.18	29900	727.95	774.46	641.96	549.13	428.94	284.4	185.8	131.3	184.9	308.6	468.9	687.26
V0144010	LE GIFFRE A TANINGES (PRESSY)	925.7	2132.51	325	8.53	9.72	13.33	21.10	35.28	38.77	30.03	19.25	15.83	14.00	12.79	10.54
V0222010	L' ARVE A ARTHAZ-PONT-NOTRE-DAME	903.82	2135.42	1664	41.49	45.69	56.40	78.12	114.55	123.6	107.9	84.23	64.61	55.34	50.60	47.97
V1264010	LE FIER A VALLIERES	878.03	2106.49	1350	44.94	51.42	55.19	64.62	60.20	41.29	24.79	15.64	24.74	36.20	44.45	48.16
V2322010	L' AIN A CERNON (VOUGLANS)	855.94	2160.68	1120	58.07	62.91	57.03	50.01	40.09	29.76	19.12	14.28	25.90	38.63	54.64	64.12
V4214010	LA DROME A LUC-EN-DIOIS	846.73	1962.41	194	3.50	3.90	4.03	4.09	3.44	1.77	0.80	0.40	0.66	1.53	2.94	3.28
V5064010	L' ARDECHE A ST-MARTIN-D'ARDECHE	776.54	1926.16	2240	99.90	85.37	67.38	62.47	62.94	30.18	12.64	13.00	39.30	103.0	108.8	85.11
W0000010	L' ISERE A VAL-D'ISERE	963.72	2060.37	46	0.45	0.41	0.43	0.64	2.03	4.90	5.16	3.34	1.79	1.13	0.74	0.59
W0224010	LE DORON DE BOZEL A LA PERRIERE	932.17	2058.89	330	5.48	5.26	5.91	8.36	18.31	26.46	27.06	21.69	13.84	10.14	7.77	6.29
W2714010	LA ROMANCHE A MIZOÛN	903.14	2011.61	220	1.49	1.45	2.43	5.09	14.04	18.75	17.04	12.40	6.70	4.91	3.20	1.90
W2764010	LA ROMANCHE AU BOURG-D'OISANS	886.43	2019.68	1000	18.86	20.55	21.81	29.88	53.82	73.69	70.43	51.87	34.85	30.72	24.91	20.33
X0310010	LA DURANCE A EMBRUN	929.803	1958.818	2170	20.81	19.72	26.06	44.04	105.94	132.6	82.02	47.43	39.79	41.67	33.39	24.03
X0434010	L' UBAYE A BARCELONNETTE	944	1940.95	549	3.40	3.32	4.84	9.18	24.27	30.11	14.44	6.46	6.11	8.09	6.40	3.90
X0454010	L' UBAYE AU LAUZET-UBAYE	923.57	1947.202	946	7.49	7.25	11.35	20.75	49.80	54.84	26.83	12.86	12.50	17.79	15.24	8.93
X0500010	LA DURANCE A ESPINASSES	913.894	1948.917	3580	33.27	32.08	44.16	74.51	173.43	202.9	114.9	63.64	56.10	67.20	55.71	38.07
X2202010	LE VERDON A DEMANDOLX	937.993	1884.295	655	8.24	8.81	13.61	21.35	31.05	19.35	7.15	4.53	5.76	12.42	14.15	9.29
Y2015010	L' ARRE AU VIGAN	706.12	1889.6	159	9.00	7.77	6.36	6.17	5.41	2.59	1.19	1.00	2.10	6.06	7.76	7.46
Y2554010	L' ORB A VIEUSSAN	652.51	1837.04	905	35.09	36.32	32.14	28.57	23.11	12.21	7.47	6.03	10.11	21.86	26.33	33.92
Y5615020	LE LOUP A GOURDON (LOUP-AMONT)	974.3	1868.7	140	3.04	3.11	3.25	3.09	2.56	1.37	0.59	0.47	0.74	2.56	3.44	2.56
Y6432010	LE VAR A MALAUSSENE (LA MESCLA)	990.542	1890.608	1830	30.22	27.94	34.33	44.72	67.03	54.52	29.83	21.50	23.70	39.34	40.84	29.69

Table 2-1 (cont.)

2.2 Meteorological dataset

2.2.1 Circulation and Weather Patterns

The Hess-Brezowsky Grosswetterlagen large-scale classification (Hess and Brezowsky, 1977) was used by Stahl (2001) to describe daily atmospheric Circulation Patterns CP. The classification is based on the geopotential height field of the 500 hPa level and the sea-level air-pressure above the North-Atlantic/European area, and defines 29 separate CPs (plus one undefined CP). These CPs form 10 major sub-types and may be assembled into four main weather type categories (Table 2-2) according to the direction of frontal zones, the location of high and low pressure areas and their rotation. Locally-designed weather classifications, such as the automatic classification defined by Bénichou (1995) focusing on France, could be more accurate for our application, but are not always maintained and can be difficult to access. The Grosswetterlagen classification, in contrast, can be freely downloaded: the catalogue (1881-1998) is available at <http://www.pik-potsdam.de/~uwerner/gwl/gwl.pdf> and is regularly updated (Gerstengarbe and Werner, 1999). Moreover, it is a well known and recognised classification, and could be expected to be applicable in most regions of Europe. For consistency with Stahl study and for its availability and recognition, the Grosswetterlagen classification was used here.

Circulation type		Description		
Major type	Subtype	N	Name	CP
Zonal circulation	W	1	West anticyclonic	Wa
		2	West cyclonic	Wz
		3	Southern West	WS
		4	Angleformed West	WW
Mixed circulation	SW	5	Southwest anticyclonic	SWa
		6	Southwest cyclonic	SWz
	NW	7	Northwest anticyclonic	NWa
		8	Northwest cyclonic	NWz
	HM	9	Central European high	HM
		10	Central European ridge	BM
	TM	11	Central European low	TM
Meridional circulation	N	12	North anticyclonic	Na
		13	North cyclonic	Nz
		14	North, Iceland high, anticyclonic	HNa
	NE	15	North, Iceland high, cyclonic	HNz
		16	British Isles high	HB
		17	Central European trough	TRM
		18	Northeast anticyclonic	NEa
		19	Northeast cyclonic	NEz
	E	20	Fennoscandinavian high anticyclonic	HFa
		21	Fennoscandinavian high cyclonic	HFz
		22	Norwegian Sea – Fennoscandinavian high, anticyclonic	HNFa
		23	Norwegian Sea – Fennoscandinavian high cyclonic	HNFz
	S	24	Southeast anticyclonic	SEa
		25	Southeast cyclonic	SEz
		26	South anticyclonic	Sa
27		South cyclonic	Sz	
28		British Isles low	TB	
29		Western Europe trough	TRW	
Unclassified	U	30	Classification not possible	U

Table 2-2: Circulation Patterns after Hess & Brezonksy (1977)

2.2.2 Rainfall and temperature

Twenty five daily rainfall and temperature data series (from *tu.tiempo.net*) were examined to link synoptic meteorology and surface hydrology (Table 2-3), selected to provide a good geographical coverage and to represent most of the range of climates observed in France (Figure 2-1 b). The period of record starts in January 1994 and ends the 31st of December 2005. Because of the relatively short record length compared to streamflow data, the complete series 1994-2005 was considered for model calibration.

Station	LAT (°)	LONG (°)	Elevation (m.a.s.l.)	Average daily temperature (°C)	Average annual rainfall (mm/yr)
ABBEVILLE	50.13	1.83	74	10.7	790
AGEN	44.18	0.6	61	13.3	660
ALENCON	48.43	0.11	144	11.1	770
AMBERIEU	45.98	5.33	250	11.6	1050
ANGERS	47.48	-0.56	57	12.3	700
AUCH	43.68	0.6	125	13.0	650
AURILLAC	44.88	2.41	640	10.2	1110
AUXERRE	47.8	3.55	207	11.5	750
BALE-MULHOUSE	47.6	7.51	270	10.8	780
BIARRITZ	43.46	-1.53	75	14.5	1290
BREST	48.45	-4.41	99	11.6	1140
CHAMBERY / AIX-LES- BAINS	45.63	5.88	235	11.7	1150
CLERMONT-FERRAND	45.78	3.16	332	12.0	570
DIJON	47.26	5.08	222	11.2	740
EMBRUN	44.56	6.5	876	10.3	590
GENEVE	46.25	6.13	420	10.8	980
GRENOBLE / ST. GEOIRS	45.36	5.33	384	11.6	820
LILLE	50.57	3.1	48	11.1	680
MARSEILLE / MARNIGNANE	43.45	5.23	6	15.5	520
METZ / FRESCATY	49.08	6.13	190	11.0	640
MONT AIGOUAL	44.11	3.58	1565	5.4	1700
MONTPELLIER	43.58	3.96	5	15.3	650
NICE	43.65	7.2	4	15.8	730
PERPIGNAN	42.73	2.86	43	15.9	520
TOULOUSE / BLAGNAC	43.63	1.36	152	13.8	590

Table 2-3: Dataset of meteorological time series

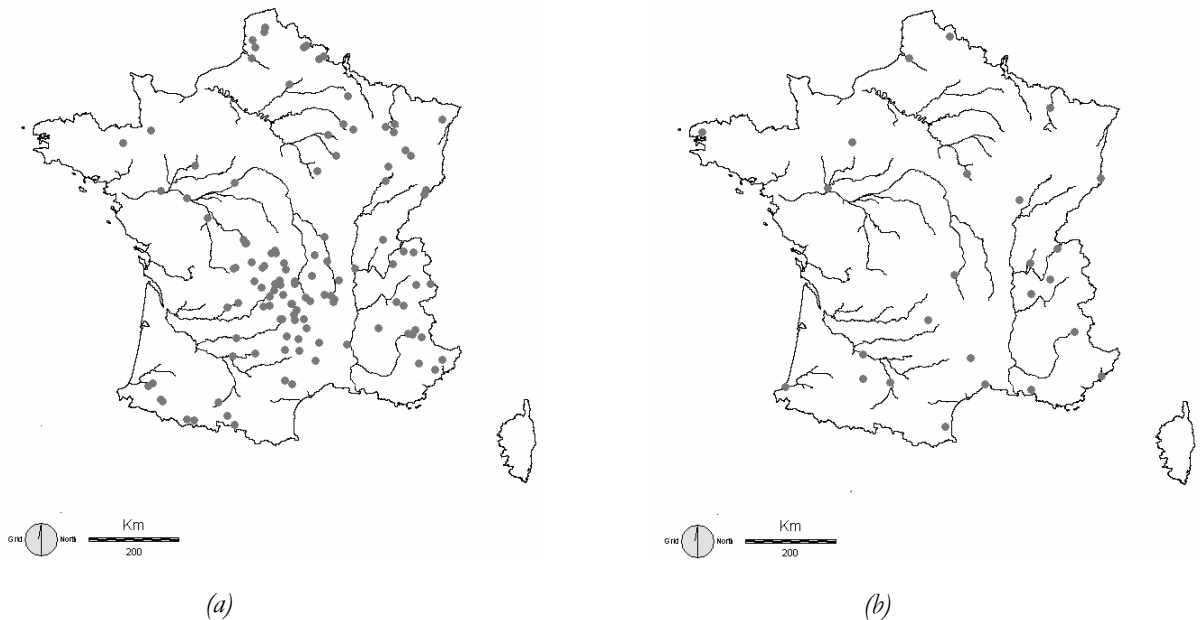


Figure 2-1: Location of the gauging stations (a) and the meteorological stations (b)

3 Deriving RDI time series

3.1 Deficiency Index Time series

To derive the flow-duration-curves, the size of the time window ($2D+1$) for extraction should be defined (cf. 1.1). D was fixed from 5 days by Stahl (2001) up to 15 days (window = 31 days) by Zaidman *et al.* (2001), but it was recommended to use at least 300 values to derive a complete flow duration curve, i.e. for 30 years record, a sampling time window of at least 10 days. In order to account for potential gaps in the record, a time window of 31 days was chosen here. The flow duration curves for day J were calculated selecting all the discharges in the time window $[J-15; J+15]$ for all of the years of record for each of the 221 gauging stations.

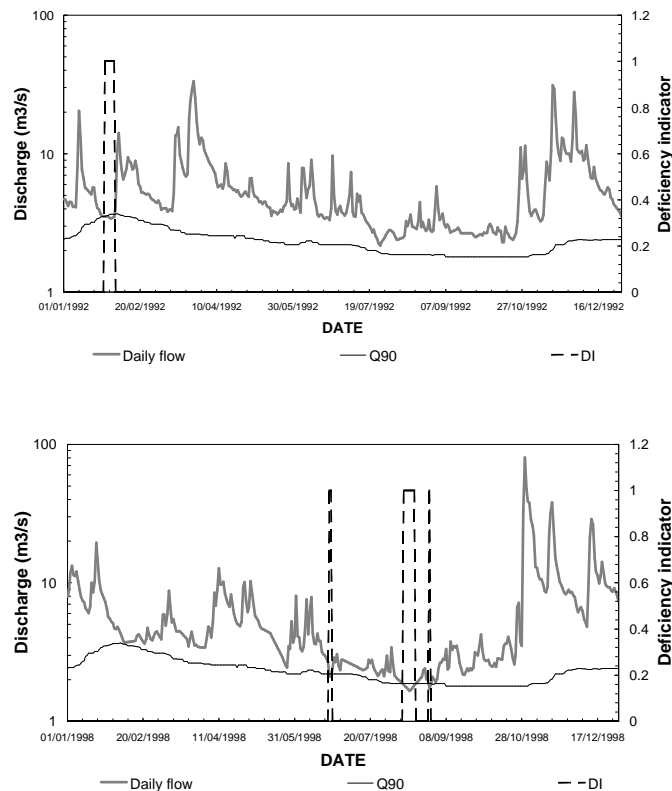


Figure 3-1: Daily flow (grey), Q_{90} (black) and DI (dashed line) for A3472010 (Zorn River @ WALTENHEIM-SUR-ZORN)

An example of daily deficiency indicator time series is given in Figure 3-1, where seasonal deficiency can be seen in summer (1998) and in winter (1992).

3.2 RDI clusters

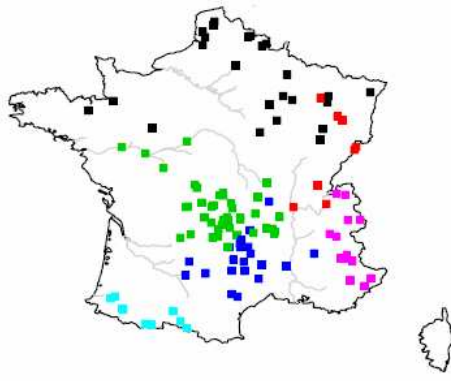
Classification was performed using two agglomerative clustering procedures: a hierarchical method found to be a more robust version of K-means method; and a partitioning method (chapter 2 and 5 in Kaufman and Rousseeuw (1990)). These two methods were coded in R language, can be freely downloaded from <http://www.r-project.org/> and are respectively named *PAM* and *AGNES* within the Cluster R-package hereafter.

At every step of the agglomeration procedure, a homogeneity criterion is calculated, that measures the spread within the cluster compared to the dissimilarity with the other clusters. A jump in this measure reflects that two ‘different’ clusters have been pooled together. One independent measure is to calculate how well a cluster is defined in terms of its *RDI* series. For that, the absolute difference for each cluster between the cumulative frequency of *RDI* (or the area underneath the curve called *RDI_{area}*) with its theoretical value (equal to 0.9 by definition) is calculated. Small departure from the theoretical value can be interpreted as a criterion of cluster homogeneity. This measure, not included within the clustering algorithm, is an independent evaluation of the clustering. However, without objective definition of a threshold for defining homogeneity, it is difficult to use. Another measure of cluster homogeneity is based on the silhouette that represents the ratio between the variations within each cluster and the variations with the other clusters. Let us consider one station *i* affected to the cluster *K*. The average distance between *i* and the remain stations of *K*, $dist(i; K)$, can be calculated, as well as the distance between *i* and the nearest cluster, $b(i)$ ($b(i) = \min[dist(i; G), G \neq K]$). This calculation is repeated for each station of *K*, and the silhouette width given by:

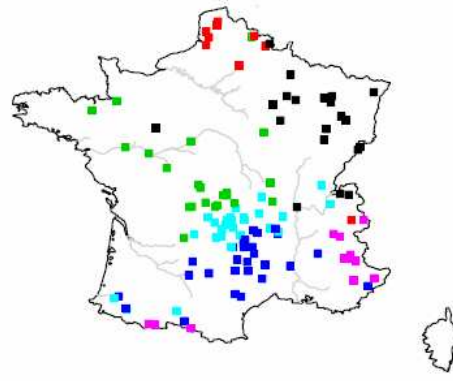
$$\text{Equation 11} \quad s(i) = (b(i) - dist(i; K)) / \max(dist(i; K), b(i))$$

Catchments with a silhouette width close to 1 are well clustered, a silhouette width around zero means that the catchment lies between two clusters, and catchments with a negative silhouette width may be located in the wrong cluster. The R-package also gives the group related to $b(i)$ as an alternative for each station.

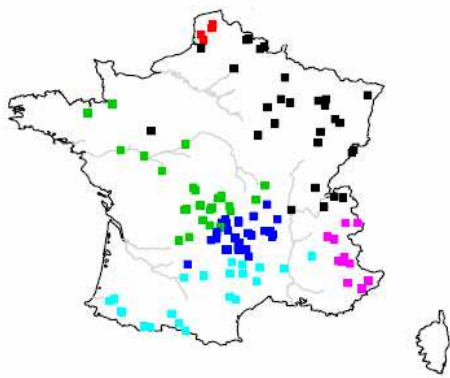
Analysis of persistence (or stationarity) of the clusters over different record periods was considered for the final definition of the regions. For three periods of record (1965-200; 1965-1990; 1975-2000), the same clustering procedure was applied, defining sets of optimal clusters, and the silhouette width calculated. Results showed that no method provided a classification that was stationary in time, and that the hierarchical algorithm (*PAM*) resulted generally in cluster less consistent in space (Figure 3-2). The partitioning technique (*AGNES*) was thus favoured and used as basis of the clustering, the silhouette width *s* exploited to finalise the clusters.



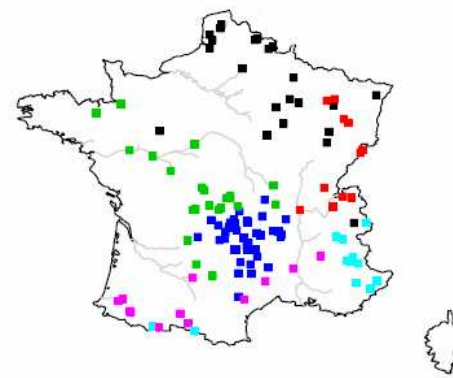
AGNES – 1965-2000



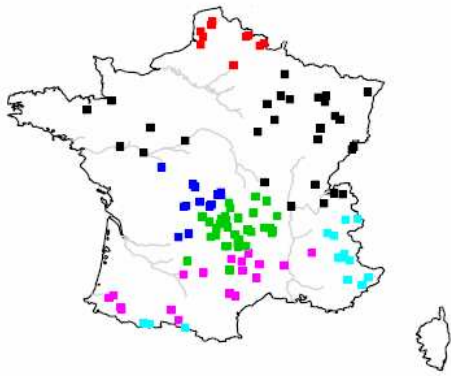
PAM – 1965-2000



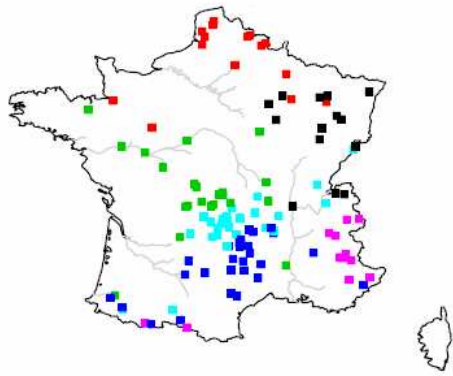
AGNES – 1965-1990



PAM – 1965-1990



AGNES – 1975-2000



PAM – 1975-2000

Figure 3-2: Maps of the 6-cluster solution for different observation periods

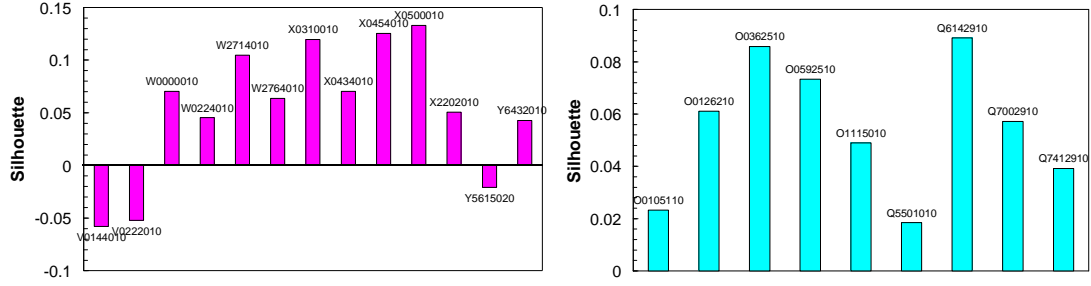


Figure 3-3: Silhouette profiles from AGNES for Alps (left) and Pyrenees (right)

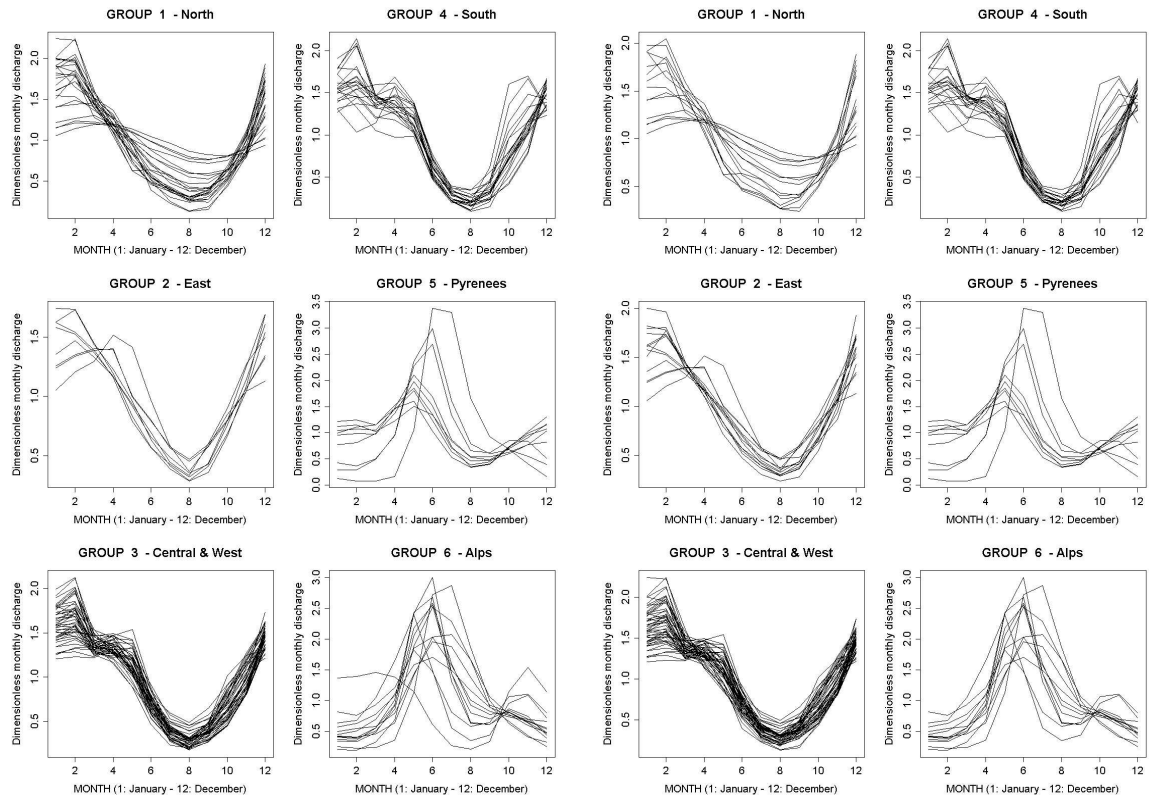
Figure 3-3 shows the silhouette profile of two AGNES groups, one that has led to a reformulation of the group (Alps), where the station Y5615020 was moved towards the South region (suggested group), due to its negative silhouette value and considering its rain-fed hydrological regime, inconsistent with the river flow regime of most stations of the Alp region. At the opposite, the Pyrenees group remained unchanged (positive silhouette for all stations).

For 28 catchments, the silhouette values were under 0.01. Twelve of the catchments were re-located to their nearest cluster. The move towards the nearest cluster was done when better homogeneity in mean monthly runoff pattern within each new group was obtained or when the geographical extent of the groups was reduced (Table 3-1). For the remaining 16 catchments, no alternative region was found, and the stations were left in the group recommended by the clustering algorithm.

Group number	Region name	Number stations
1	North	14
2	East	13
3	Central & West	51
4	South	22
5	Pyrenees	9
6	Alps	12

Table 3-1: Final regions

Figure 3-4 shows the runoff pattern in each group according to AGNES (observation period 1965-2000) and for the modified and final clusters (regions). A better consistency in the mean monthly river flow regime characterises the final regions. Figure 3-5 shows the spatial distribution of the six clusters (to be compared to Figure 3-2 AGNES 1965-2000).



(a) *AGNES*

(b) *Final groups*

Figure 3-4: Runoff pattern in each class defined by *AGNES* clustering procedure (a), and final regions (b)

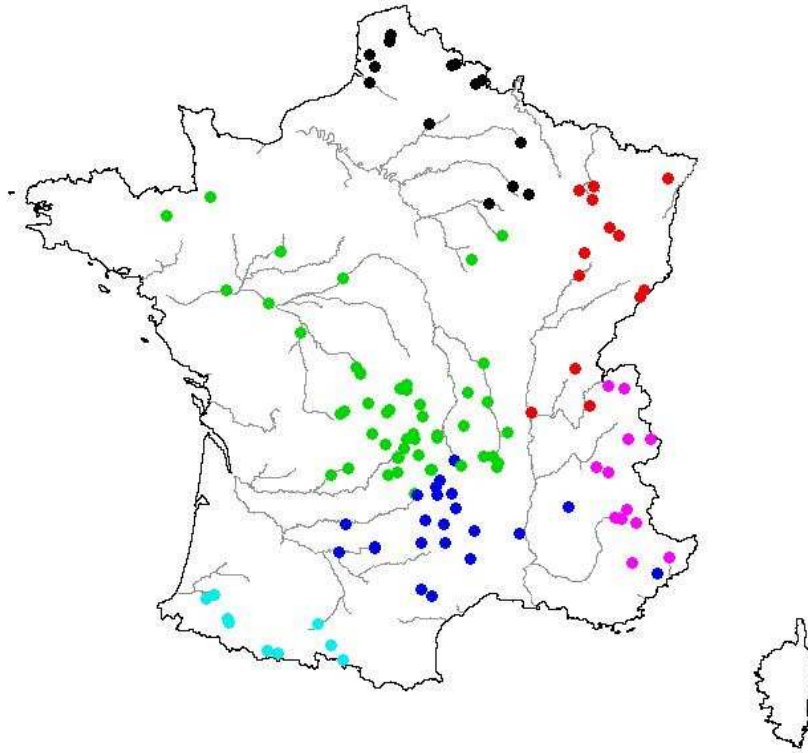


Figure 3-5: Location of the final clusters (black North Region 1; red East Region 2; green Central & West Region 3; dark blue South Region 4; cyan Pyrenees Region 5; magenta Alps Region 6)

3.3 Explanatory analysis

As mentioned previously, *RDI* time series contain a large proportion of zero. As a consequence, the time series are highly auto-correlated. Auto-correlation (ACF) is the strongest for North (Region 1) with ACF greater than 0.5 up to 97-days, due to the control of the surface runoff by groundwater (Figure 3-6 left), and the smallest for Alps (Region 6) with ACF greater than 0.5 up to 17 days. The transformation of *RDI* in y removes a large part of this autocorrelation (Figure 3-6 right) as well as some of the asymmetry characterising *RDI* (Figure 3-6 (b) compared to (a)).

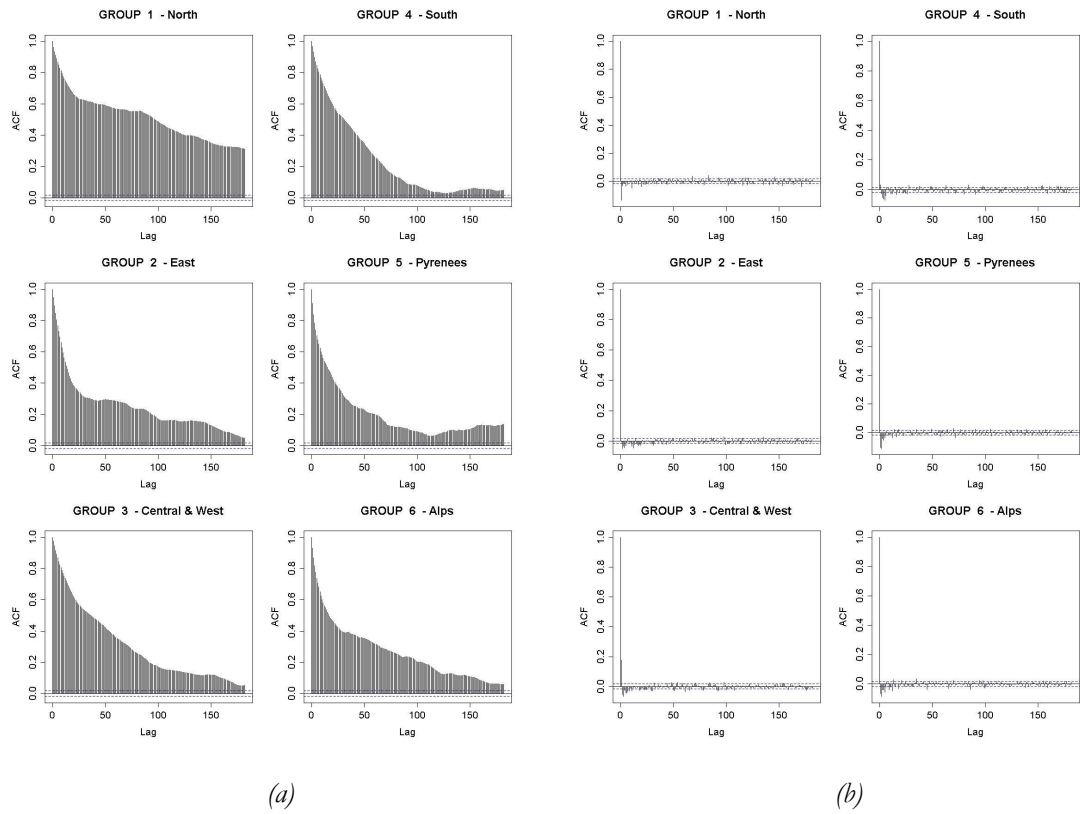


Figure 3-6: Autocorrelation of RDI (a) and y (b) for each region

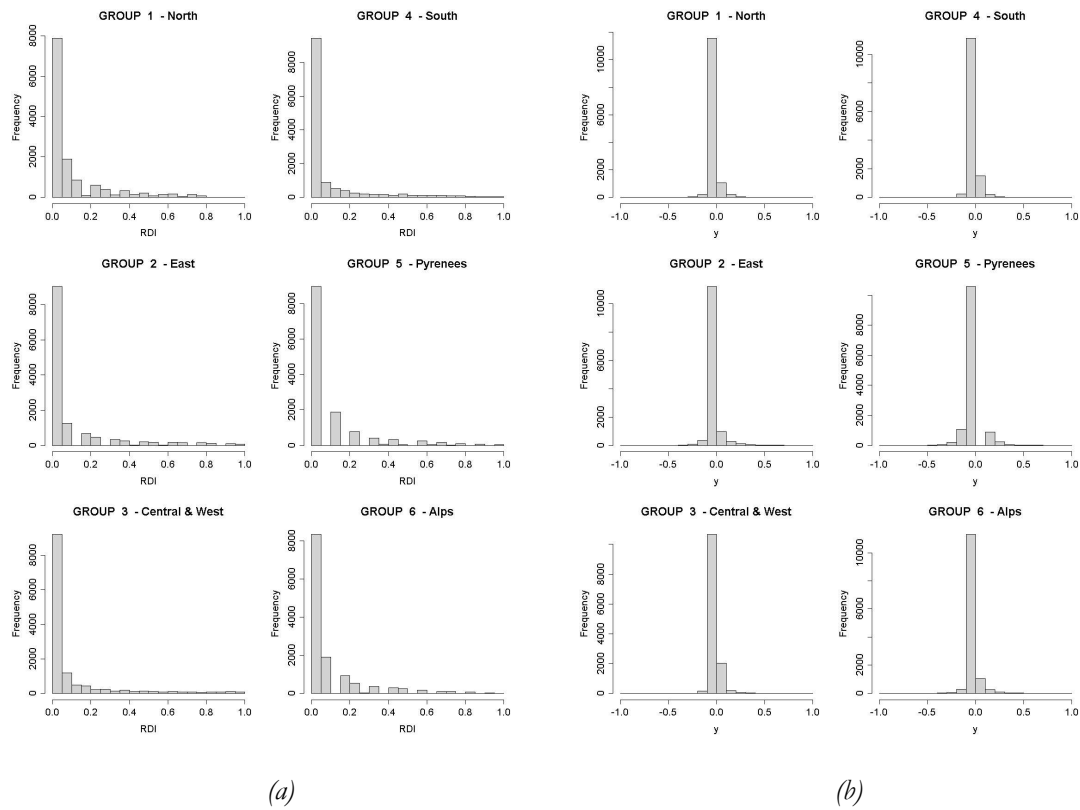


Figure 3-7: Histogram of RDI (a) and y (b) for each region

The cumulative distribution of *RDI* for each region illustrates the homogeneity within the cluster. In theory, if all the stations behaved in the same way, *RDI* should contain 90% of zero and 10% of 1. Figure 3-8 compares the expected distribution (black dotted lines) to the observed (solid line). All the regions show the same level of heterogeneity, with the smoothest curve observed for the region with the largest size (Central and West region, group 3).

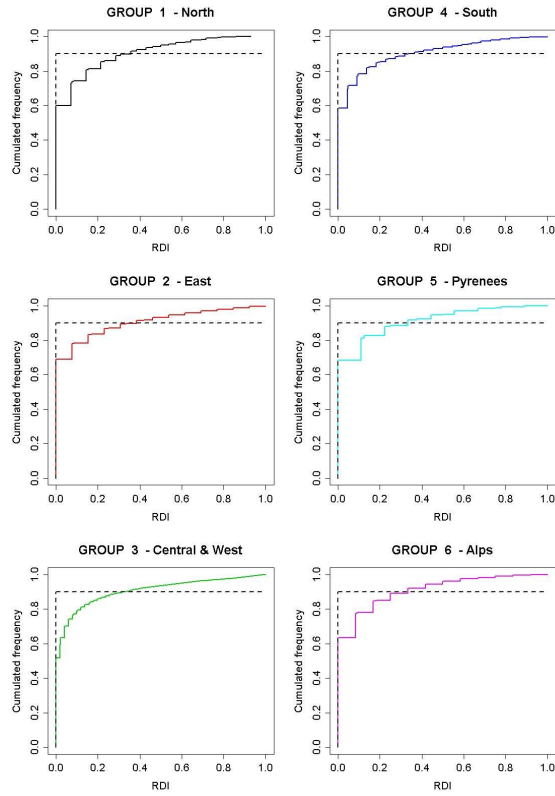


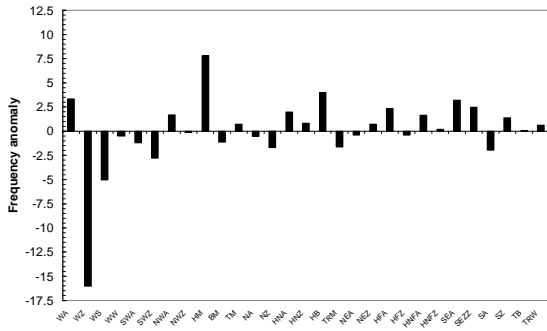
Figure 3-8: Cumulative frequency distribution of RDI for each region

4 Modelling of RDI after Stahl 2001

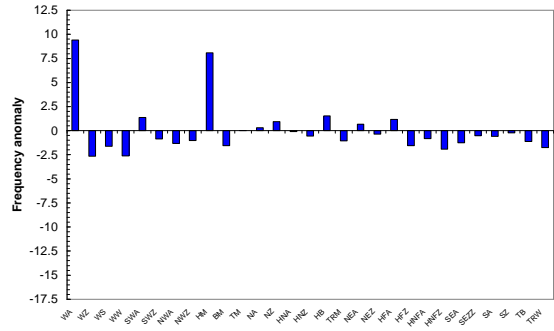
4.1 Weather type groups: CP groups

Stahl (2001) suggested to define Circulation Patterns groups (CP groups) according to their frequency anomalies related to streamflow deficiency. She investigated the anomalies associated with severe regional deficiency periods (as defined with $RDI > 0.3$), with and without lags (i.e. CP occurring x days previous RDI value). The same CP showed the largest negative or positive anomalies for most regions (West cyclonic Wz and central European High HM), but significant regional differences were also highlighted. Anomalies generally peaked at less than 10 % for simultaneous anomalies (i.e. 10% of the time when the given weather type occurred, the region had RDI greater than 0.3), but dropped to around 3% for 30-day lagged anomalies. When calculated on seasons, the anomaly signals proved stronger and more region-specific and thus recommended to use (Stahl, 2001). The CP anomalies were then used to define seasonal groups of CP to be linked with RDI , with a maximum of nine groups possible, to avoid problems due to some CP occurring much less often than others (c.f. 1.4). However, note that this procedure does not guaranty CP groups to be consistent with the rainfall pattern associated with their weather types.

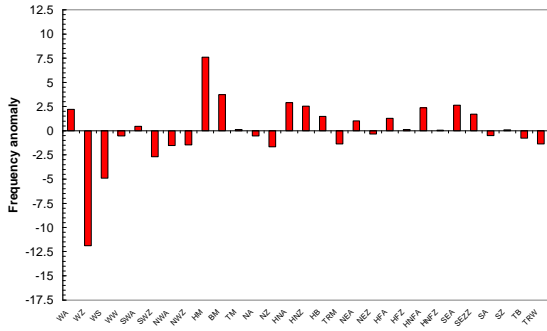
Applied to the 6 regions defined in France in 3.2, CP groups were obtained per season (Table 4-1), with seasons defined as winter (December to February), spring (March to May), summer (June to August), and autumn (September to November).



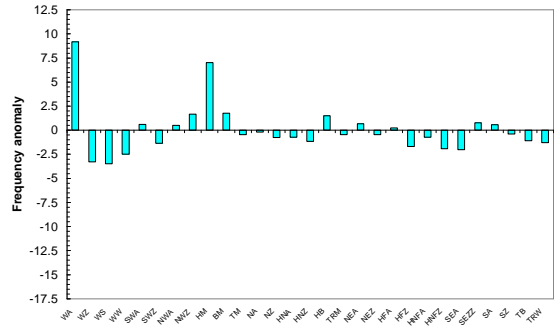
(a) Region 1 North



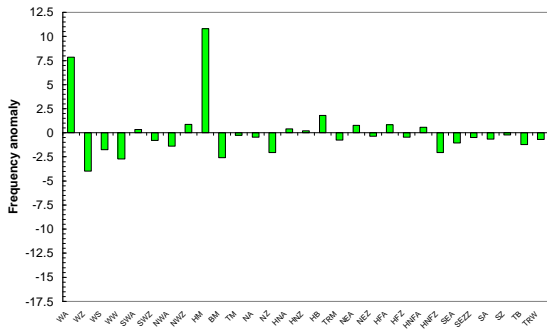
(d) Region 4 South



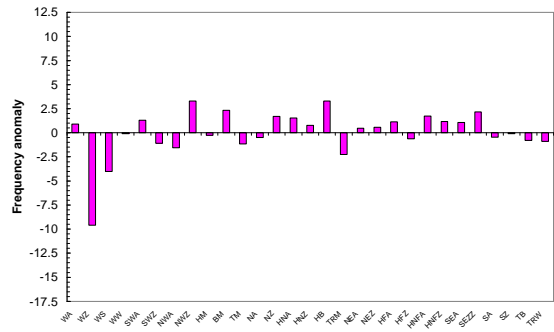
(b) Region 2 East



(e) Region 5 Pyrenees



(c) Region 3 Central & West



(f) Region 6 Alps

Figure 4-1: Frequency anomaly during RDI>0.3 for each region in winter

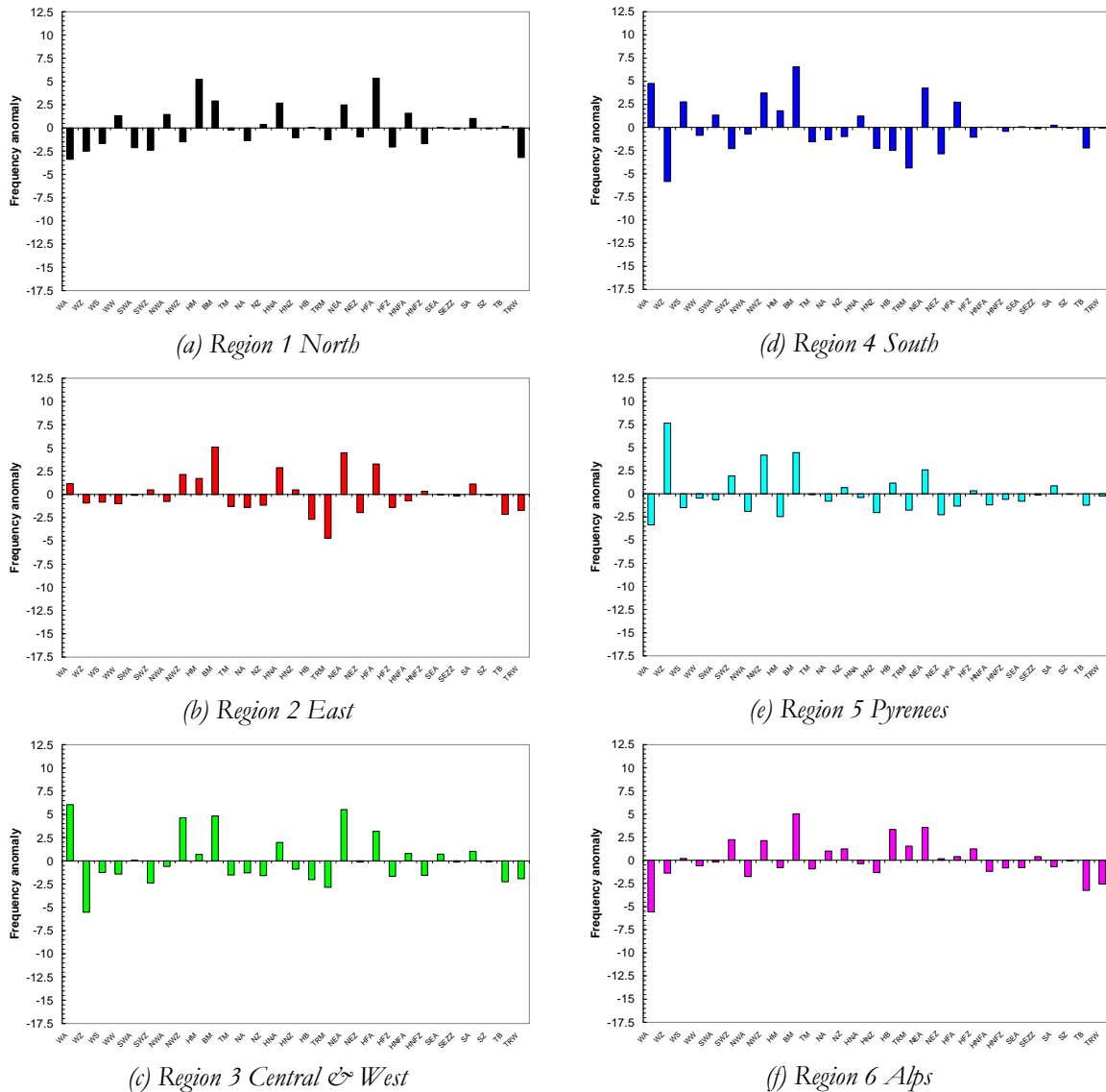


Figure 4-2: Frequency anomaly during $RDI > 0.3$ for each region in summer

There is only a few weather type associated with the largest frequency anomalies (categories 1-2 or 8-9 in Table 4-1), the great majority showing anomalies of $\pm 2\%$ (categories 4 to 6) (Figure 4-1 and Figure 4-2). Anomalies are smallest in summer. Wa, HM and BM weather types generally show positive anomalies, i.e. they occur more frequently than usual during days of severe drought ($RDI > 0.3$), for all regions and seasons. Western weather types (Wz, WS and SWz) occur less frequently than usual during severe droughts, as indicated by their negative frequency anomalies. Other weather types have more regional and seasonal variations, such as TB and TRW, generally (but not always) associated with negative anomalies, or BM and HB (both positive and negative anomalies). Regional variations in the groupings of weather types are found to be smaller than seasonal variation (compare the difference between winter and summer frequency anomalies in Figure 4-1 and Figure 4-2 to variations for a same season but all regions), but they do exist (e.g. SWz shows strong positive anomalies all seasons but summer, when it shows strong negative anomalies in all regions Table 4-1). However, the grouping technique

does not take into account the actual occurrence frequency, and it may be possible that some of the frequency anomalies values are biased by a very small occurrence of an individual weather type. Results are consistent with those of Stahl (2001).

GWL	North				East				Central & West				South				Pyrenees				Alps			
	winter	spring	summer	autumn	winter	spring	summer	autumn	winter	spring	summer	autumn	winter	spring	summer	autumn	winter	spring	summer	autumn	winter	spring	summer	autumn
Wa	3	3	7	3	3	4	4	3	2	2	2	3	2	3	3	3	2	2	7	2	4	6	8	2
Wz	9	4	7	7	9	7	6	8	7	6	8	8	7	6	8	7	7	7	2	6	8	7	6	7
WS	8	7	6	5	7	6	6	6	6	7	6	7	6	7	3	7	7	5	6	6	7	5	5	7
WW	6	6	4	4	6	6	6	6	7	6	6	7	7	6	6	7	7	6	5	7	5	4	6	6
SWa	6	3	7	7	5	5	5	6	5	3	5	4	4	3	4	4	4	4	6	3	4	6	5	4
SWz	7	6	7	7	7	7	4	7	6	6	7	7	6	6	7	7	6	7	4	6	6	7	3	7
NWa	4	5	4	5	6	5	6	3	6	4	6	2	6	4	6	2	5	5	6	2	6	4	6	5
NWz	5	7	6	6	6	7	3	4	4	6	3	4	6	4	3	4	4	6	3	5	3	7	3	4
HM	2	4	2	3	2	4	4	3	1	3	4	2	2	2	4	3	2	4	7	3	5	5	6	3
BM	6	4	3	8	3	3	2	6	7	3	3	2	6	3	2	2	4	5	3	7	3	6	2	6
TM	4	7	5	6	5	7	6	6	5	7	6	6	5	7	6	6	5	3	5	6	6	2	6	6
Na	6	4	6	5	6	6	6	4	5	4	6	5	5	4	6	5	5	4	6	5	5	6	4	4
Nz	6	4	5	3	6	6	6	4	7	5	6	3	4	6	6	6	6	6	4	3	4	3	4	4
HNa	4	3	3	5	3	3	3	5	5	3	4	5	5	3	4	4	6	3	5	4	4	6	5	6
HNz	4	6	6	5	3	6	4	4	5	5	6	6	6	4	7	6	6	4	7	5	4	3	6	5
HB	3	3	5	3	4	3	7	2	4	4	7	3	4	4	7	3	4	5	4	4	3	5	3	2
TRM	6	7	6	5	6	7	7	6	6	5	7	6	6	4	7	6	5	6	6	6	7	4	4	7
NEa	5	5	3	5	4	3	3	5	4	4	2	5	4	4	3	5	4	5	3	5	5	5	3	5
Nez	4	3	6	4	5	4	6	6	5	6	5	6	5	6	7	5	5	5	7	6	4	3	5	4
HFa	3	7	2	4	4	3	3	4	4	5	3	5	4	7	3	5	5	6	6	6	4	5	5	4
HFz	5	4	7	5	5	4	6	6	5	5	6	6	6	4	6	6	6	5	5	6	6	5	4	6
HNFa	4	2	4	4	3	3	6	4	4	3	4	5	6	6	5	6	6	5	6	5	4	6	6	4
HNFz	5	7	6	6	5	5	5	5	7	6	6	5	6	6	5	5	6	6	6	6	4	4	6	5
SEa	3	3	5	6	3	3	5	6	6	6	4	7	6	6	5	7	7	6	6	5	4	5	6	6
SEZz	3	6	5	5	4	6	5	5	5	6	5	6	6	6	5	6	4	4	5	6	3	4	5	5
Sa	6	6	4	5	6	6	4	5	6	6	4	6	6	6	5	6	4	6	4	6	5	6	6	6
Sz	4	6	5	5	5	5	5	5	5	6	5	6	5	5	5	6	5	5	5	5	5	6	5	6
TB	5	7	5	4	6	6	7	6	6	7	7	7	6	6	7	6	6	6	6	5	6	7	7	7
TRW	4	7	7	4	6	6	6	7	6	7	6	7	6	7	5	7	6	4	5	7	6	7	7	5

Table 4-1: CP groups for each region

4.2 RDI modelling

Table 4-2 lists the best parameter set, and corresponding Pearson coefficient and index of agreement (c.f. 1.5) for the six regions using up to nine CP groups. The Pearson correlation coefficient (goodness-of-fit used to select the best parameter set) ranges from 0.516 (East) to 0.622 (North) while the index of agreement (independent index) varies from 0.691 (South) to 0.740 (North). The coefficients associated with CP groups 1 to 4 are all positive; those associated with CP groups 6 to 9 are negative. This is consistent with the group definition, where CP

groups 1 to 4 are formed of weather types occurring more often than normal during days of severe drought (positive frequency anomalies, c.f. 4.1), thus expected to be associated with an increase of the *RDI*. CP group 5, which is formed of weather types with no significant anomalies during severe droughts, have positive (North and Alps) or negative (East and Central & West) coefficients.

While the results are not very good, they are of the same order of magnitude or slightly better than results obtained by Stahl (2001). For Alpine regions (c11 and c12), Pearson coefficient was, for the calibration period, of 0.391 and 0.428 respectively, while we achieved a value of 0.516. South Jura (c17 in Stahl) only had a 0.473 Pearson coefficient, compared to 0.516 for East. Spain (c18) had only a 0.399 Pearson, compared to 0.500 for Pyrenees. However, regions with high density of stations in Stahl (2001), such as West Germany (c8) and South East UK (c2) showed a better correlation between simulated and observed *RDI* in Stahl's study than the closest French regions (East and North). Note the difference in the calibration periods, Dec 1971 - May 1987 in Stahl, Jan 1965 – Dec 2000 here.

Region	CPGroup1	CPGroup2	CPGroup3	CPGroup4	CPGroup5	CPGroup6	CPGroup7	CPGroup8	CPGroup9	γ_0	R Pearson	σ
North	-	0.065	0.0585	0.0103	0.0091	-0.0367	-0.0426	-0.0042	-0.0638	0.5039	0.622	0.740
East	-	0.0197	0.0443	0.0111	-0.0232	-0.0046	-0.0935	-0.0445	-0.0993	-0.7002	0.516	0.713
Central & West	0.1307	0.0311	0.0343	0.0229	-0.0187	-0.0240	-0.1461	-0.0205	-	-0.9268	0.605	0.772
South	-	0.103	0.04	0.0297	-0.1037	-0.018	-0.0422	-0.055	-	0.5918	0.527	0.691
Pyrenees	-	0.0648	0.0436	0.0049	-0.0053	-0.0894	-0.015	-	-	-0.5762	0.500	0.694
Alps	-	0.0373	0.0347	0.0152	0.0018	-0.0227	-0.048	-0.0188	-	-0.7598	0.528	0.721

Table 4-2: Optimised parameters and goodness-of-fit measures for RDI modelling of the six regions using up to 9 weather type groups based on seasonal weather type occurrences during severe drought periods

5 A CP clustering based on rainfall occurrence

5.1 New CP clustering

The application of the approach developed by Stahl (2001) to France giving relatively poor results, a different methodology for clustering the weather types was developed. The main hypothesis is that atmospheric circulation pattern mostly influences *RDI* evolution through rainfall. Groups of weather types can be formed using strong relationship between weather types and rainfall amounts, rather than uniquely dependant on anomaly frequencies relative to *RDI* values.

To establish these links, let us consider three main weather types, expected to have strong influence on the weather in France. CP-type Ws is characterized by depressions shifted from southwest Ireland to France and central Germany. Low pressure may extend up to northeast Mediterranean. Ws would thus be expected to be associated with rainfall across France. CP-type HM is characterized by an extended high pressure system in central Europe. Depressions are blocked in Eastern Atlantic and Russia. The probability of rain during HM days is thus expected to be low. CP-type Wz is the West cyclonic type with low pressure over Central Europe. Contrasting situations between Northern and Southern France may be observed. Thus rainfall should be more likely to be observed in the North whereas dry conditions might prevail in the South.

In order to identify potential links, the distribution of days with more than 1 mm of rain recorded, (daily amount considered as significant) in each weather type was studied. Table 5-1 shows the mean proportion of days with more than 1 mm of rain for two stations, Lille (North) and Marseille (South), at annual and seasonal scale. The four seasons are spring (March - May), summer (June - August), autumn (September - November) and winter (December - February). This proportion varies from one weather type to another and is consistent with our interpretation of the atmospheric circulation pattern. Ws type (resp. HM) is associated with wet days (resp. dry days) both in Lille and Marseille. Wz is one of the wettest weather types in Lille and one of the driest ones in Marseille at annual and seasonal scale.

GWL	Year	Winter	Spring	Summer	Autumn	GWL	Year	Winter	Spring	Summer	Autumn
Wa	0.16	0.17	0.22	0.14	0.13	Wa	0.09	0.06	0.04	0.06	0.17
Wz	0.53	0.56	0.58	0.45	0.51	Wz	0.10	0.11	0.11	0.03	0.14
WS	0.52	0.48	0.43	0.00	0.67	WS	0.24	0.07	0.14	0.00	0.67
WW	0.67	0.60	0.42	0.80	0.83	WW	0.13	0.20	0.00	0.00	0.13
SWa	0.28	0.44	0.28	0.25	0.18	SWa	0.10	0.10	0.08	0.00	0.15
SWz	0.59	0.68	0.61	0.56	0.56	SWz	0.14	0.12	0.17	0.05	0.19
NWa	0.13	0.12	0.11	0.05	0.17	NWa	0.06	0.04	0.00	0.00	0.09
NWz	0.36	0.46	0.29	0.31	0.35	NWz	0.04	0.06	0.04	0.05	0.00
HM	0.04	0.04	0.04	0.05	0.02	HM	0.04	0.07	0.03	0.00	0.04
BM	0.18	0.18	0.16	0.16	0.25	BM	0.11	0.12	0.07	0.06	0.24
TM	0.43	0.00	0.35	0.59	0.46	TM	0.16	0.00	0.29	0.06	0.09
Na	0.17	0.17	0.25	0.00	0.00	Na	0.03	0.17	0.00	0.00	0.00
Nz	0.48	0.64	0.29	0.39	0.52	Nz	0.08	0.15	0.08	0.06	0.00
HNa	0.09	0.04	0.06	0.17	0.09	HNa	0.20	0.36	0.09	0.00	0.41
HNz	0.48	0.40	0.59	0.47	0.29	HNz	0.14	0.00	0.18	0.12	0.29
HB	0.05	0.08	0.00	0.07	0.07	HB	0.10	0.13	0.11	0.02	0.27
TRM	0.51	0.52	0.54	0.45	0.52	TRM	0.16	0.19	0.23	0.08	0.15
NEa	0.04	0.00	0.25	0.00	0.00	NEa	0.15	0.00	0.25	0.19	0.00
Nez	0.32	0.20	0.31	0.27	0.60	Nez	0.03	0.00	0.08	0.00	0.00
HFa	0.11	0.05	0.06	0.14	0.19	HFa	0.18	0.31	0.06	0.10	0.23
HFz	0.20	0.33	0.00	0.21	0.50	HFz	0.12	0.17	0.08	0.11	0.25
HNFa	0.12	0.00	0.12	0.22	0.07	HNFa	0.23	0.33	0.22	0.11	0.30
HNFz	0.29	0.17	0.60	0.20	0.35	HNFz	0.39	0.52	0.20	0.40	0.29
SEa	0.16	0.05	0.09	0.27	0.25	SEa	0.39	0.50	0.42	0.08	0.42
SEZz	0.40	0.25	0.56	0.46	0.20	SEZz	0.43	0.47	0.44	0.36	0.40
Sa	0.24	0.11	0.25	0.39	0.26	Sa	0.27	0.28	0.20	0.15	0.33
Sz	0.43	0.38	0.25	0.00	0.50	Sz	0.61	0.88	0.50	0.00	0.50
TB	0.57	0.17	0.68	0.42	0.65	TB	0.22	0.17	0.16	0.23	0.28
TRW	0.50	0.45	0.51	0.54	0.47	TRW	0.33	0.35	0.34	0.13	0.54

(a) Lille

(b) Marseille

Table 5-1: Proportion of days with more than 1 mm rain at Lille (a) and Marseille (b)

Figure 5-1 illustrates the link between Lille and Marseille rainfall at annual scale. The proportion of days with more than 1 mm rainfall associated with each CP weather type is replaced by its corresponding rank (1 for the driest CP weather-type, 30 for the wettest). Spearman's coefficient Rho is close to zero (0.16) indicating weak correlation between the two stations.

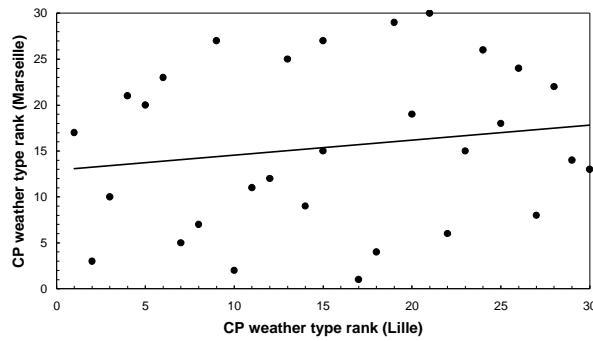


Figure 5-1: Correlation between the two meteorological stations Lille and Marseille

Two main conclusions can be drawn. First the difference in proportion of rainy days between CP classes justifies clustering CP weather types according to the rainfall occurrence. Second, the clustering process should be carried out at regional scale to account for spatial variability. Difference in wet and dry weather types with season is less significant but seasonal clustering will be investigated.

The first step is to define the meteorological station representative of each region. The selection was carried out considering geographical proximity (Table 5-2). Stations related to the regions may be located in the neighbourhood of the cluster.

Region	Station
North	ABBEVILLE, LILLE, METZ
East	METZ, BALE, DIJON, AMBERIEU, GENEVE, CHAMBERY
Central & West	ALENCON, ANGERS, AURILLAC, AUXERRE, CLERMONT-FERRAND, DIJON
South	AGEN, AURILLAC, MARSEILLE, MONTAIGOUAL, MONTPELLIER, TOULOUSE
Pyrenees	AGEN, AUCH, BIARRITZ, PERPIGNAN, TOULOUSE
Alps	GENEVE, EMBRUN, NICE, GRENOBLE

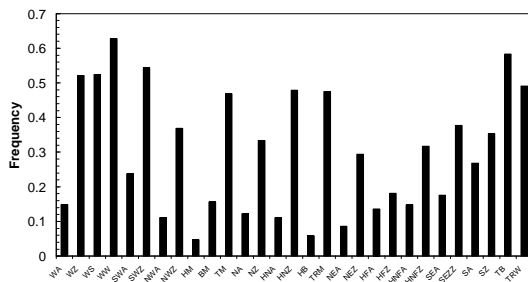
Table 5-2: Meteorological stations included in the clustering process for weather type groups definition

The second step consists in calculating the frequency of rainy days for each CP weather type. Figure 5-2 displays these frequencies for each CP weather type at annual scale for each region. They range from 0.04 to 0.65 with a median value close to 0.30. Regions in the North and the East exhibit more variability than Southern areas (East and Pyrenees). Graphic identification of regional differences is difficult.

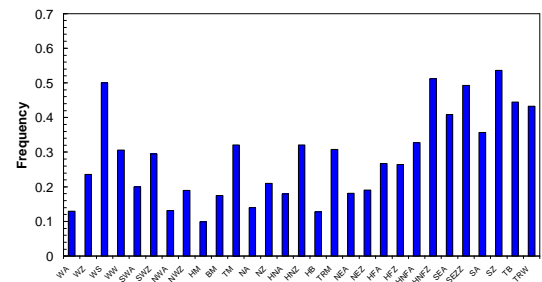
Region	North	East	Central & West	South	Pyrenees	Alps
North	1.000	0.934	0.879	0.646	0.686	0.791
East	-	1.000	0.941	0.778	0.818	0.927
Central & West	-	-	1.000	0.894	0.897	0.940
South	-	-	-	1.000	0.949	0.912
Pyrenees	-	-	-	-	1.000	0.926
Alps	-	-	-	-	-	1.000

Table 5-3: Spearman's coefficient (Rho) between regions

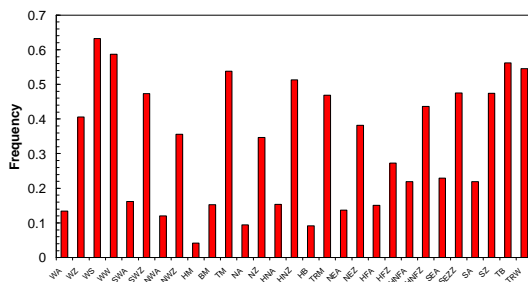
Spearman's coefficient (Rho) between regions based on the annual frequency of rainy days by CP weather type have been computed to provide an indication of these differences (Table 5-3). The smallest value is observed for the pair North-South but is higher (above 0.6) than the value calculated for the two meteorological stations Lille-Marseille (0.16). The spatial contrast is reduced due to the “smoothness” effect when considering regional variables.



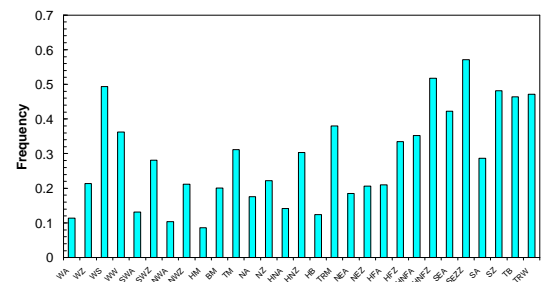
(a) Region 1 North



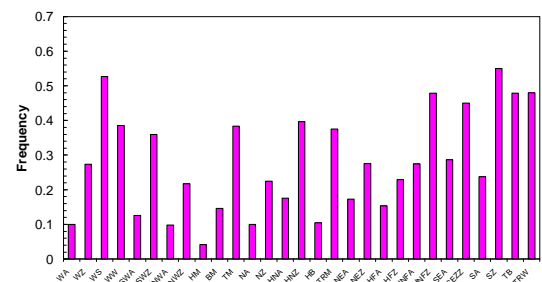
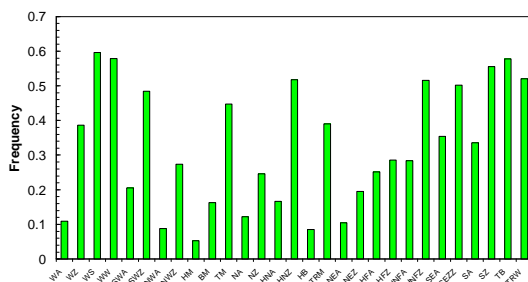
(d) Region 4 South



(b) Region 2 East



(e) Region 5 Pyrenees



(c) *Region 3 Central & West*

(f) *Region 6 Alps*

Figure 5-2: *Proportion of days with rainfall amount of more than 1 mm for each region (annual scale)*

The new clustering process is based on the occurrence of rain days during each weather types. The weather types are ordered according to the frequency of rainfall days they are associated with. The lowest frequencies indicate weather types linked with less rain days (i.e. ‘dry’ types) while the highest frequencies characterise weather types more generally associated with rain (i.e. ‘wet’ types). Weather type groups are defined, that have similar overall frequency of occurrence within the analysed period (year or season). This is to avoid disproportionate weight for weather types with very low occurrence, that is possible in Stahl’s methodology. First, the driest CP weather type was combined with the dry dry CP weather types until reaching approximately a total frequency of occurrence equal to $1/n$, where n is the number of final clusters. The first group (dry) was set up, including m CP weather types. The same procedure was applied considering the $(m+1)^{th}$ CP weather type as starting point for aggregation. The number CP weather types in each cluster varies from one group to another. The same clustering technique was repeated looking at both seasonal and annual rainfall frequencies to build the new weather types groups.

GWL	North				East				Central & West			
	winter	spring	summer	autumn	winter	spring	summer	autumn	winter	spring	summer	autumn
Wa	3	3	2	3	2	3	2	2	2	2	2	2
Wz	8	8	6	8	6	6	6	6	6	7	6	6
WS	6	8	1	8	8	8	1	8	8	8	8	1
WW	8	5	8	8	8	5	7	8	8	6	6	5
SWa	4	5	5	2	3	3	4	2	3	4	4	4
SWz	8	7	8	7	8	7	7	7	7	8	7	8
Nwa	2	1	1	2	1	3	4	1	1	4	4	1
NWz	6	4	5	5	8	5	6	4	5	4	4	4
HM	1	1	1	1	1	1	1	1	1	1	1	1
BM	3	3	3	4	3	2	4	3	3	3	3	3
TM	4	5	8	5	4	7	8	6	7	7	8	8
Na	2	3	1	1	1	1	4	1	3	1	1	1
Nz	5	4	4	5	5	5	4	5	4	4	4	4
HNa	2	3	2	1	4	3	1	1	3	3	2	2
HNz	5	8	6	4	7	8	7	7	7	8	7	7
HB	1	1	1	1	1	2	1	2	1	1	2	2
TRM	5	7	7	6	7	7	8	7	5	7	7	7
NEa	1	4	1	1	1	6	1	1	1	4	2	2
Nez	2	5	4	6	4	5	8	5	1	5	4	4
HFa	2	2	4	3	3	1	2	3	4	4	4	4
HFz	4	1	4	4	3	4	6	3	8	1	5	5
HNFa	1	3	4	1	3	4	4	4	3	5	7	7
HNFz	4	5	6	4	4	5	8	8	4	8	8	8
SEa	1	1	5	4	4	3	4	4	4	3	6	6
SEZz	4	5	8	2	7	5	8	5	5	7	8	8
Sa	2	5	5	4	2	5	4	4	3	5	7	7
Sz	4	4	1	4	7	6	1	7	8	7	1	1
TB	4	8	8	8	4	8	7	8	8	8	8	8
TRW	5	6	8	5	4	8	8	8	8	8	8	8

Table 5-4: Rain-based CP groups for each region

The first model considers eight groups. Eight groups configuration is the closest analogy to the 9 CP-groups clustering suggested by Stahl, so that results can be compared. Results are displayed with eight groups (Table 5-4). Clusters are globally stable from one season to another. Variations in seasonal CP weather types grouping may be due to the small numbers of a certain CP weather type during a given season, leading to a change in the number of occurrences of rainy days for that weather type. Differences between seasonal clusters are manifest for the Pyrenees region. For the other regions, the clustering process leads to group approximately the same CP weather types whatever the season is.

5.2 RDI modelling

The same method of estimation of the CP group coefficients as described in 1.5 and applied in 4.2 is used here. Results (Table 5-5) are of the same order of magnitude that the ones obtained using Stahl's clustering procedure (Table 4-2, p. 33). The highest score (Pearson coefficient and coefficient of agreement) is found for North (respectively 0.638 and 0.796), and the lowest for the Alps (respectively 0.437 and 0.647). The sensitivity to the clustering procedure seems weak. It may improve slightly the performance (North region). The lowest values are observed in the mountainous areas (Pyrenees and Alps regions). The actual performance of the models will be tested on an independent observation period in the next section.

Ra	CP	Ra	CP	Ra	CP	Ra	CP	Ra	CP	Ra	CP	Ra	CP	y_0	R	
in-based	group 1	in-based	group 2	in-based	group 3	in-based	group 4	in-based	group 5	in-based	group 6	in-based	group 7	in-based	group 8	Pearson
																0.638
0.030		0.022		0.009		0.004		-0.015	0.008	0.053		0.026		0.53		
0.085		0.054		0.007		0.013		0.02							0.32	0.508
								0.055	0.063	0.056						
0.071		0.002		0.050		0.036		-0.075							0.28	0.575
								0.045	0.022	0.730						
0.014		0.060		0.018		-0.012		-0.006	0.020	0.106		0.056		0.72		0.523
0.0255		0.052		0.002		0.0107		0.0079								
								0.064	0.0343	0.0303					0.42	0.427
0.022		0.046		0.033		0.037		-0.041								0.437
								0.008	0.070	0.085		0.32-				

Table 5-5: Optimised parameters and goodness-of-fit measures for RDI modelling of the six regions using eight weather type groups based on seasonal rain occurrence

5.3 Sensitivity analysis

Sensitivity to the season of grouping (annual rather than seasonal) and to the number of final groups (four instead of eight) was investigated. In particular, considering four groups resulted in a much faster optimisation of the coefficient, the optimisation for eight groups being very time consuming.

Year-based groups are listed in Table 5-6.

WL	G	Nort	East	Cent	Sout	Pyre	Alps
		h		ral & West	h	nees	
A	W	2	2	2	1	1	1
Z	W	7	6	6	5	5	6
S	W	8	8	8	8	8	8
W	W	8	8	8	6	7	7
WA	S	4	4	3	4	2	2
WZ	S	8	7	7	6	6	7
WA	N	2	1	1	2	1	1
WZ	N	5	5	4	3	4	4
M	H	1	1	1	1	1	1
M	B	3	3	3	3	3	3
M	T	5	8	7	7	6	7
A	N	2	1	2	2	2	2
Z	N	4	4	4	4	6	4
NA	H	1	3	3	3	2	4
NZ	H	6	8	8	7	6	8
B	H	1	1	1	1	2	2
RM	T	6	7	7	7	7	7
EA	N	1	2	1	3	2	3
EZ	N	4	5	3	3	3	6
FA	H	2	2	4	6	4	3
FZ	H	4	4	5	5	6	4
NFA	H	2	4	4	7	7	6

	H	4	6	7	8	8	8
NFZ							
	S	4	4	5	8	8	6
EA							
	S	5	7	7	8	8	8
EZZ							
	S	4	4	5	7	6	4
A							
	S	4	7	8	8	8	8
Z							
	T	8	8	8	8	8	8
B							
	T	6	8	8	8	8	8
RW							

Table 5-6: Annual rain-based CP group for all regions

Results are given for a calibration period of 1965-2000. Pearson correlation coefficients range from 0.473 to 0.651. These values are of the same order than the ones calculated previously (Table 4-2, p. 33). Thus we do not identify any significant evolution in the efficiency criteria.

Ra	CP	Ra	CP	Ra	CP	Ra	CP	Ra	CP	Ra	CP	Ra	CP	Ra	CP	y ₀	R
in-based	group 1	in-based	group 2	in-based	group 3	in-based	group 4	in-based	group 5	in-based	group 6	in-based	group 7	in-based	group 8		Pearson
	0.041	0.002	-	0.02	0.025	0.055	-	0.002	0.03	0.027	-	0.2	0.651				
													0.473				
	0.073	0.064	0	0.018	0.013	0.038	0.042	0.052	0.68								
	0.052	0.036	0.011	0.022	-	-	-	-	-	0.621							
					0.044	0.006	0.140	0.144	0.72								
	0.056	0.044	-	0.046	0.025	0.008	0.036	0.145	0.096	0.44	0.579						
	0.02	0.068	0.028	0.016	-0.02	-	-	-	-	0.504							
						0.152	0.054	0.026	0.24								

Table 5-7: Optimised parameters and goodness-of-fit measures for RDI modelling of the six regions using eight weather type groups based on annual rain occurrence

Regio	Dry	MedDr	MedW	Wet	y_0	R	a
North	0.024	0.004	-	-	-	0.598	0.769
East	0.071	0.020	0.035	0.033	0.46	0.443	0.647
West	0.022	0.015	0.016	0.05	0.95	0.537	0.705
South	0.040	0.008	0.013	0.076	0.74	0.485	0.696
Pyrenees	0.015	0.001	-	0.002	0.014	0.84	0.418
Alps	0.032	0.043	0.029	0.080	0.31	0.408	0.622

Table 5-8: Optimised parameters and goodness-of-fit measures for RDI modelling of the six regions using four weather type groups based on seasonal rain occurrence

Regio	Dry	MedDr	MedW	Wet	y_0	R	a
North	0.020	0.007	0.017	0.023	0.75	0.549	0.736
East	0.057	0.008	0.020	0.039	0.73	0.463	0.660
West	0.043	0.013	0.012	0.129	0.79	0.615	0.780
South	0.050	0.027	0.016	0.112	0.38	0.535	0.715
Pyrenees	0.061	0.018	0.022	0.143	0.10	0.448	0.640
Alps	0.032	0.032	0.042	0.039	0.07	0.438	0.634

Table 5-9: Optimised parameters and goodness-of-fit measures for RDI modelling of the six regions using four weather type groups based on annual rain occurrence

In all cases, the lowest performances are observed for the mountainous areas. The difficulty of modelling may be due to the fact that temperature data is not included in the clustering process. CP weather types with precipitation are grouped without distinction between rain fall and snow fall and the severity of the drought may be reduced by the occurrence of a dry and hot day without rain but snow melt.

6 Models evaluation

The performance of all the models is assessed by comparing their ability to predict drought during the period 2001-2004, excluded from the calibration. The models are all run from the 1st January 1965 to the 31st December 2004. Year 2005 is not included in the calculation, as the number of gauging stations with complete data series reduced. The same goodness-of-fit indices as for the calibration period are calculated for the period between 01/01/2001 to 31/12/2004, i.e. coefficients of correlation (Pearson) and coefficient of agreement

RDI time series are displayed to compare graphically the models with more than seven CP weather type clusters (Figure 6-1 to Figure 6-6). “RAIN” refers to the new rain-based clustering approach and “STAHL” to the clusters of Section 4. We can note that:

- performance varies from one region to another, from one model to another. Drawing general conclusions is not easy;
- all the models in all the regions predict reasonably well the occurrence of the summer 2003 drought but not its intensity.

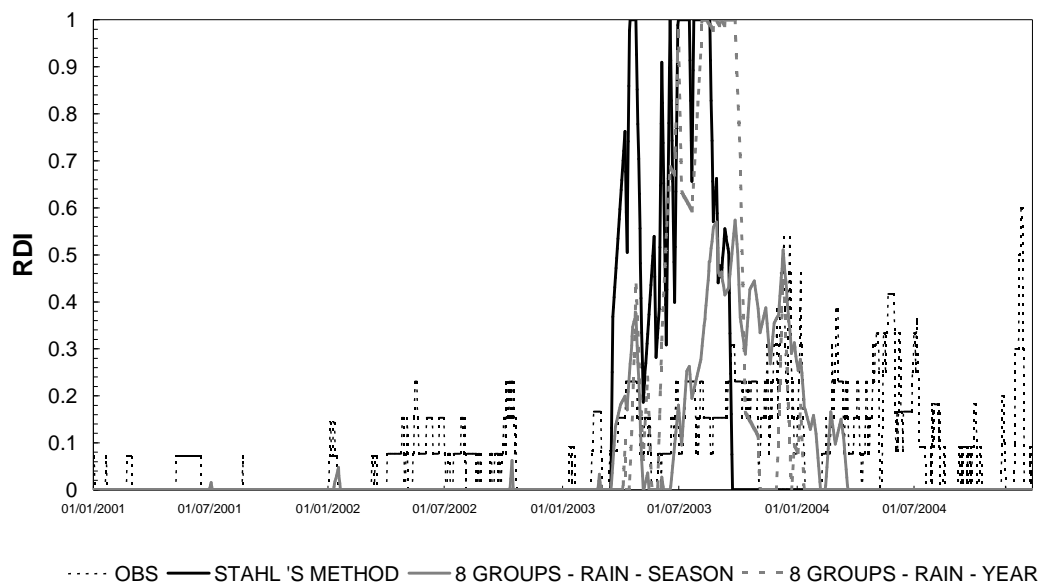


Figure 6-1: Modelled RDI for the validation period 2001-2004 – North

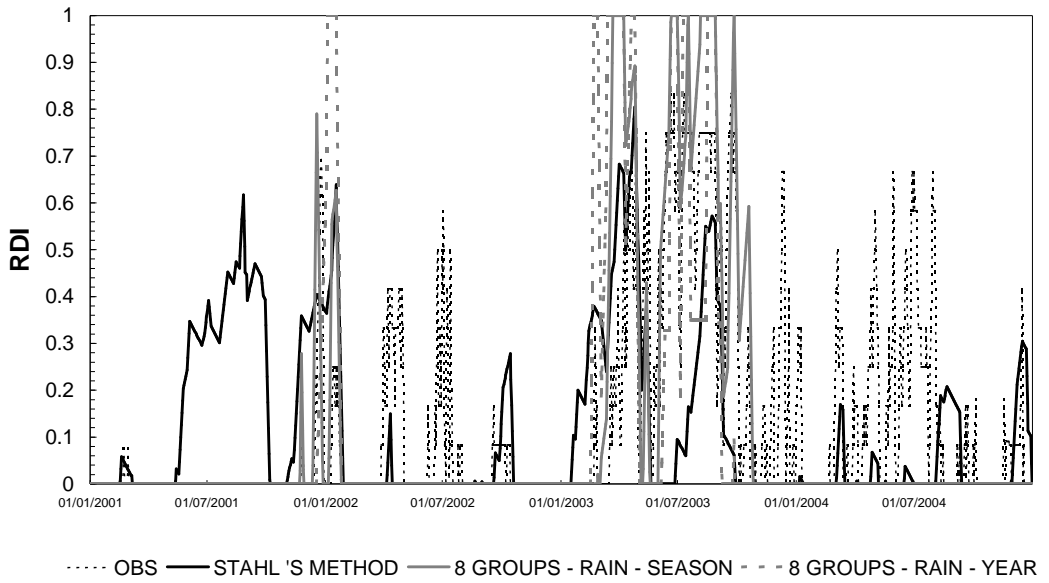


Figure 6-2: Modelled RDI for the validation period 2001-2004 – East

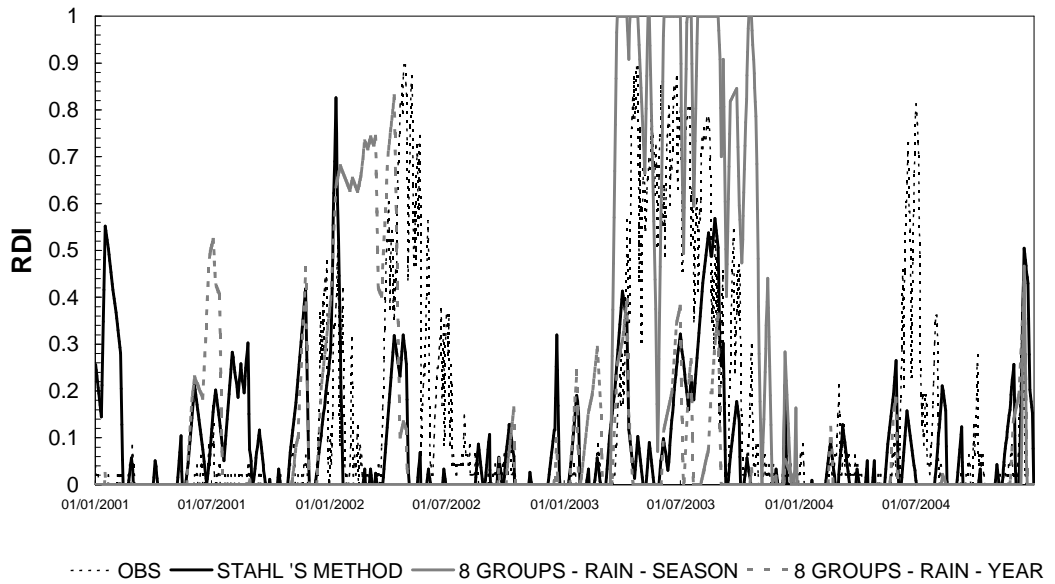


Figure 6-3: Modelled RDI for the validation period 2001-2004 – Central & West

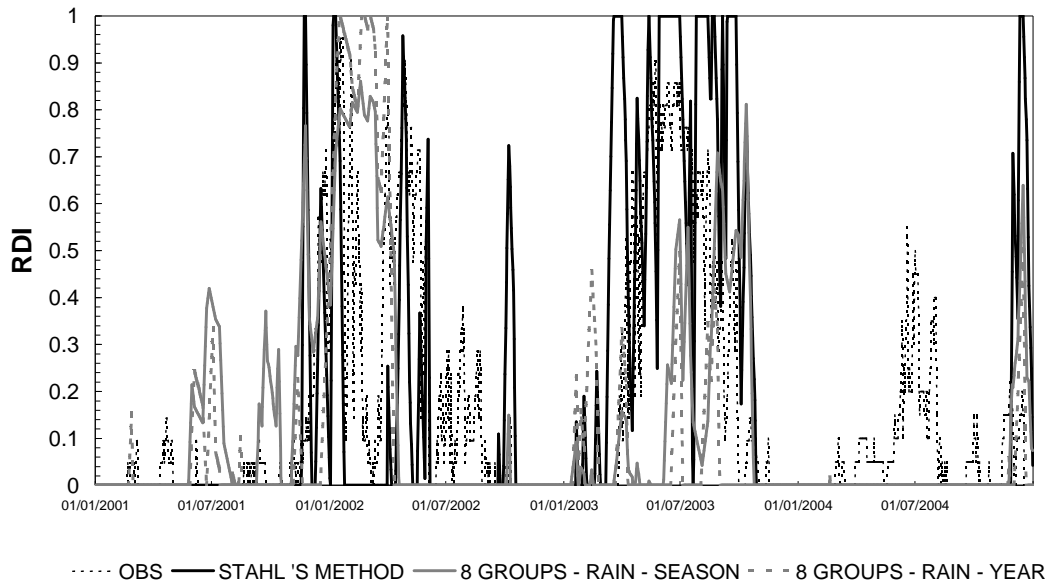


Figure 6-4: Modelled RDI for the validation period 2001-2004 – South

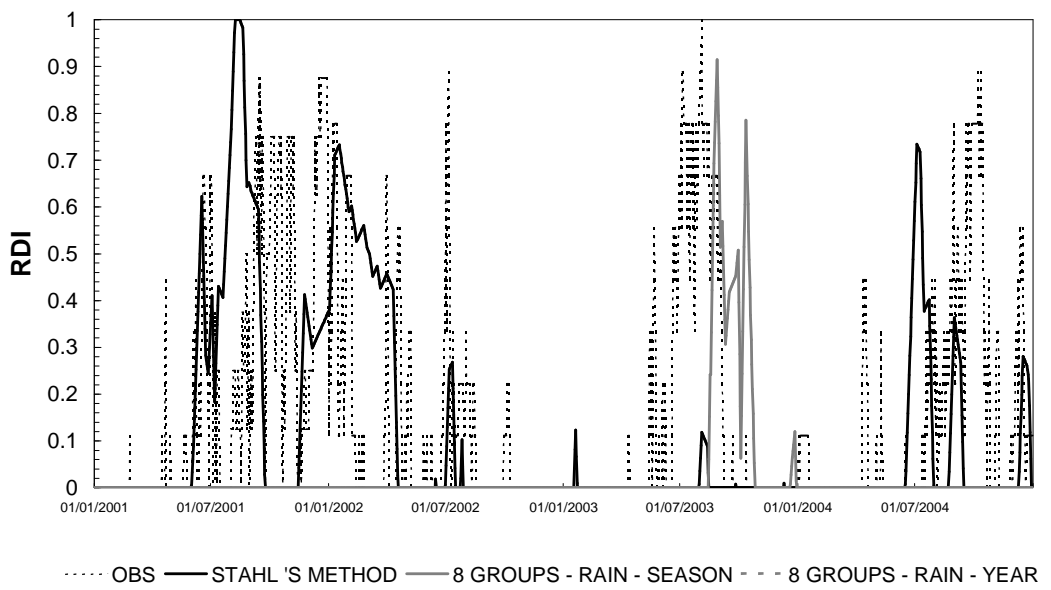


Figure 6-5: Modelled RDI for the validation period 2001-2004 – Pyrenees

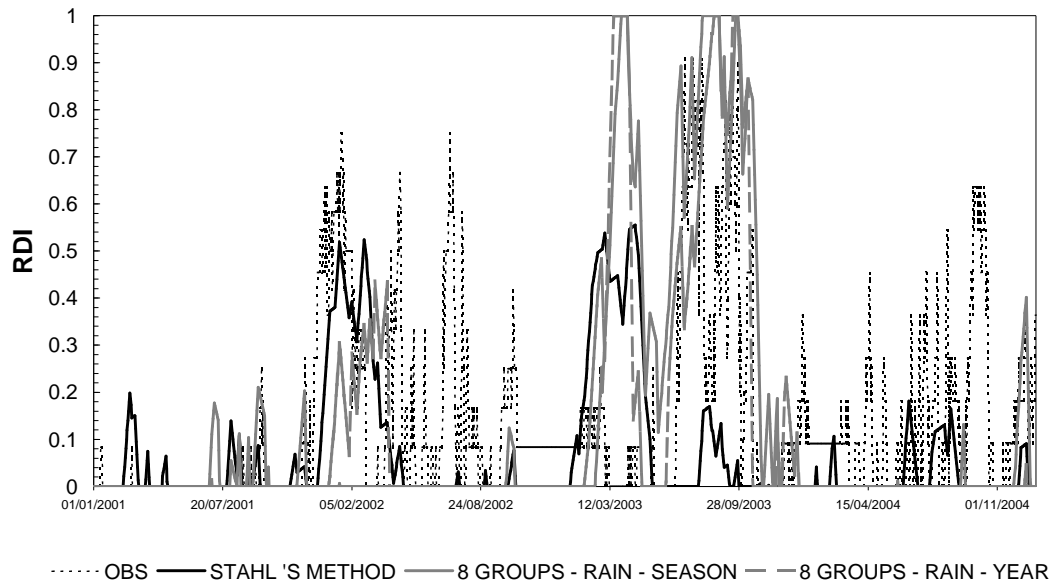


Figure 6-6: Modelled RDI for the validation period 2001-2004 – Alps

The next figures are related to the four CP weather type clusters to illustrate sensitivity to the seasonality in the clustering process.

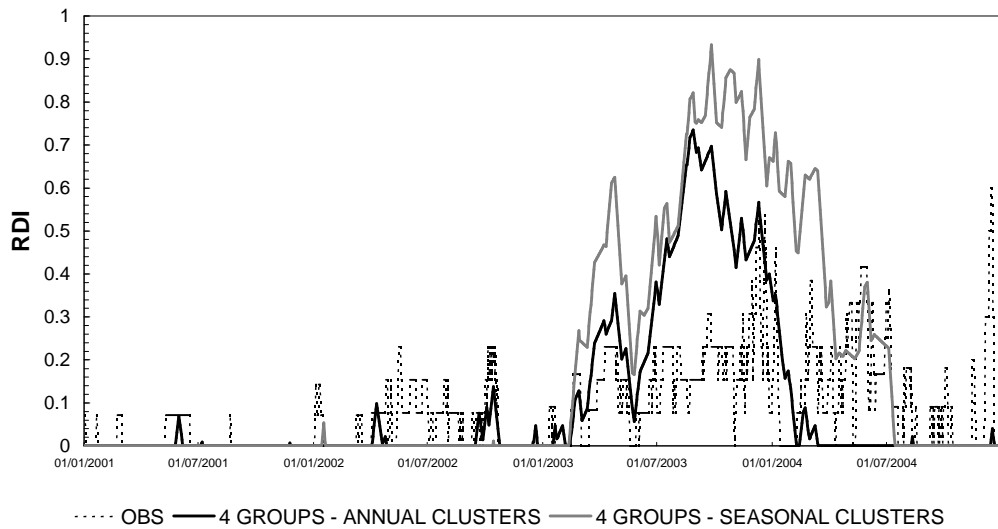


Figure 6-7: Modelled RDI for the validation period 2001-2004 – North, 4 groups

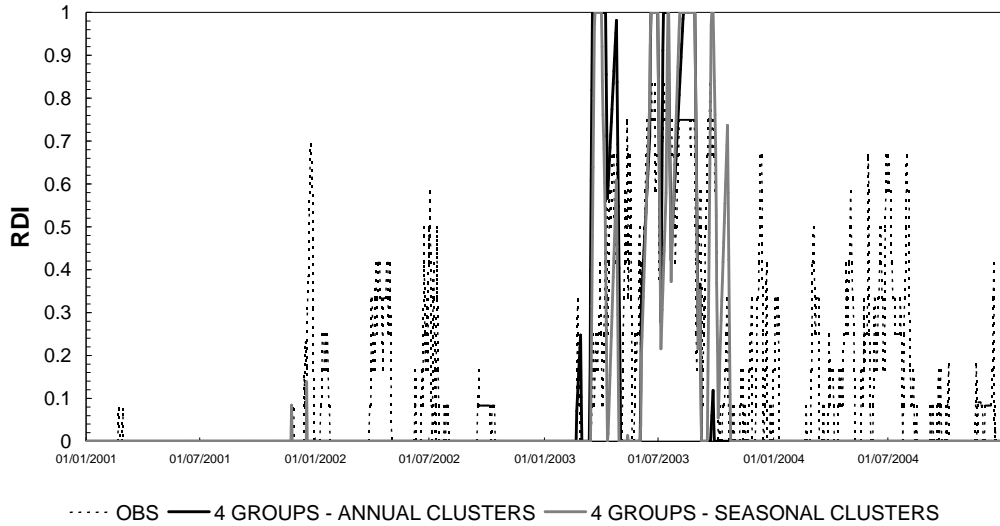


Figure 6-8: Modelled RDI for the validation period 2001-2004 – East, 4 groups

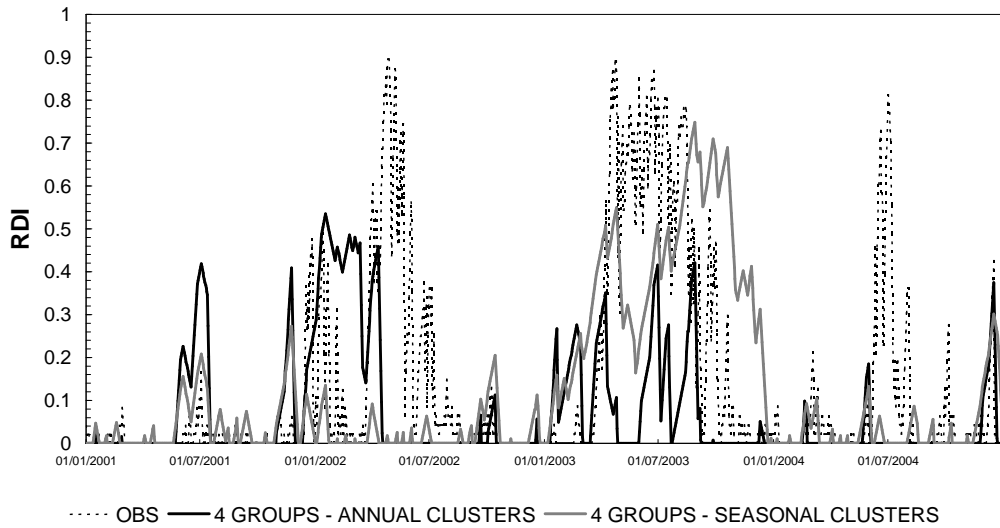


Figure 6-9: Modelled RDI for the validation period 2001-2004 – Central & West, 4 groups

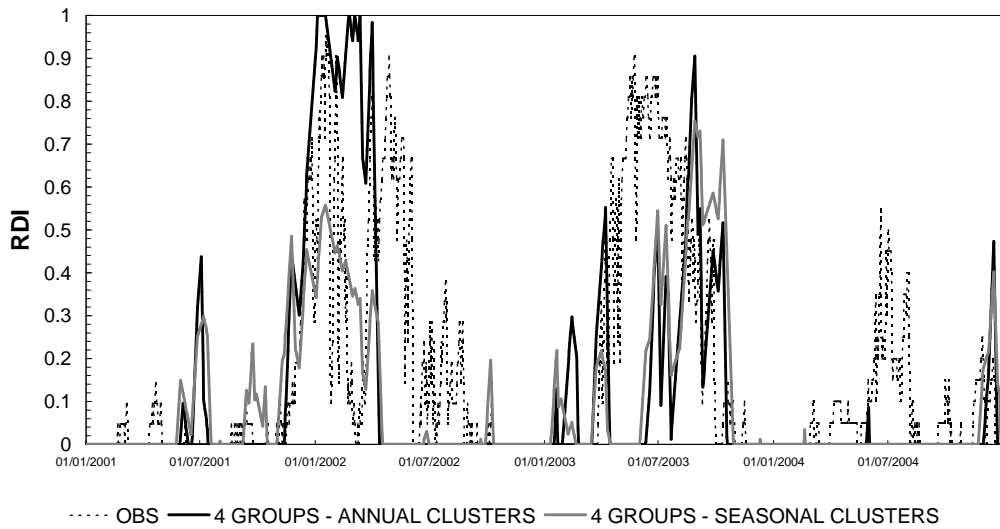


Figure 6-10: Modelled RDI for the validation period 2001-2004 – South, 4 groups

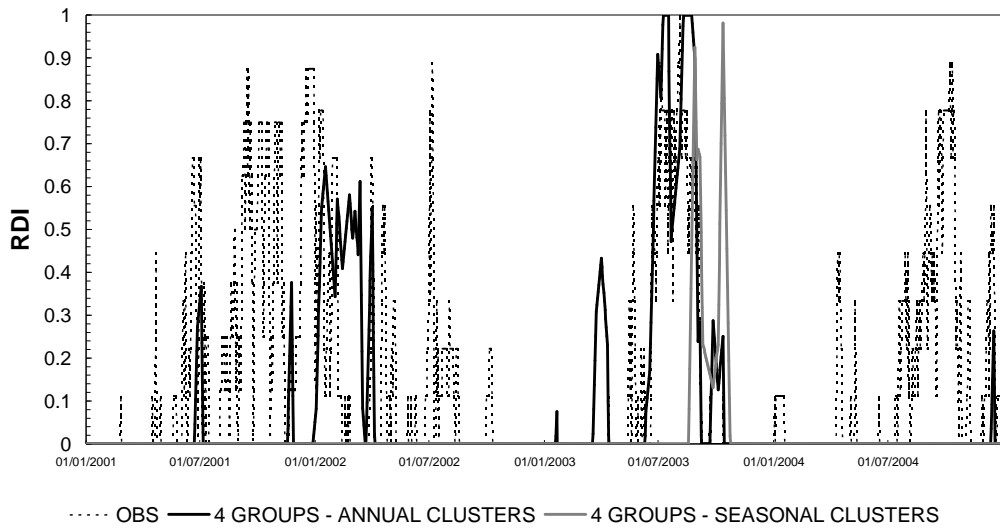


Figure 6-11: Modelled RDI for the validation period 2001-2004 – Pyrenees, 4 groups

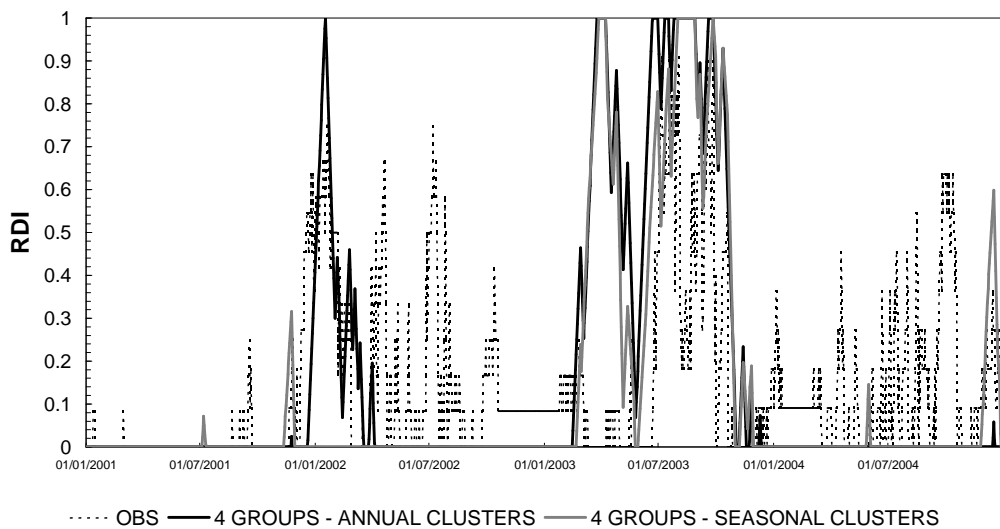


Figure 6-12: Modelled RDI for the validation period 2001-2004 – Alps, 4 groups

The same goodness-of-fit indices as used for the calibration are computed over the validation period. Rain-based grouping generally leads to larger goodness-of-fit indices than RDI-based grouping, but all performances are significantly reduced compared to the calibration period (except for South region with Stahl’s approach).

Statistics in Table 6-1 suggest that a 4-group approach is justified as it does not significantly reduce the performance in validation.

Clustering approach		TAHL	AIN	AIN	AIN	AIN
Number of clusters		9				
Time scale						
North	a	.393	.456	.710	.637	.553
	R Pearson	.235	.326	.507	.490	.592
East	a	.506	.674	.822	.774	.794
	R Pearson	.196	.473	.695	.553	.579
Central & West	a	.498	.408	.764	.411	.655
	R Pearson	.264	.093	.508	.128	.349
South	a	.775	.547	.618	.650	.624
	R Pearson	.609	.315	.372	.304	.313
Pyrenees	a	.481		.277	.633	.390
	R Pearson	.200		.052	.385	.250
Alps	a	.382	.606	.600	.667	.605
	R Pearson	.135	.248	.232	.321	.243

Table 6-1: Goodness-of-fit measures for RDI modelling of the six regions in validation (*Y* – clustering based on annual rainfall occurrence; *S* – clustering based on seasonal rainfall occurrence)

7 Discussion and conclusions

The approach suggested by Stahl (2001) for modelling a regional drought index using atmospheric circulation pattern classification was implemented in France, a region not included in Stahl's original study. The relatively poor quality of the modelling results in calibration (small percentage of variance explained) lead to investigate a new clustering process, that regroups weather types according to their association with rainfall or no rainfall, instead of being based on the occurrence of certain weather types during severe drought events. The results obtained are of the same order of magnitude as those obtained by Stahl in Europe during the calibration periods. Despite a modelling procedure that does not explicitly include any temporal dynamic (and in particular there is no accounting of the delay between the occurrence of a weather type and hydrological response of the basins), CP groups explain up to 25% of the temporal variability of *RDI*. In validation, most of the models are able to predict the summer 2003 drought.

However...

- Parameters can always be fitted but the solution may reflect a local minimum or may give weights that are not physically based (for example positive values associated to wet clusters in particular when many rain-based clusters are considered);
- At this stage, the efficiency is too poor to consider the models as useful forecasting tools;
- In addition, for the models to be used as forecasting tools, it would be necessary to first build weather types forecasts (a few months ahead), which are not yet available.

Nevertheless, some improvements could be suggested:

- Introducing logistic regression for modelling the link between hydrological drought and circulation pattern. This has already been tested in Southern Germany by (Stahl and Demuth, 1999);
- Considering four groups for the clustering of weather types, based on seasonal occurrence of CP, including both rainfall and temperature anomalies that could improve modelling in mountainous areas.

References

Bénichou, P. (1995) Classification automatique de configurations météorologiques sur l'Europe occidentale, Météo France, Toulouse.

Demuth, S. and Stahl, K. (Eds.) (2001) *ARIDE - Assessment of the Regional Impact of Droughts in Europe*, Institute of Hydrology, University of Freiburg.

Gerstengarbe, F. W. and Werner, P. C. (1999) Katalog der Großwetterlagen Europas (1881-1998) nach Paul Hess und Helmuth Brezowsky, Postdam.

Hess, P. and Brezowsky, H. (1977) Katalog der Großwetterlagen Europas 1881-1976. 3 verbesserte und ergänzte Auflage. Ber Dt. Wetterd. 15 (113).

IPCC (2001) *Climate Change 2001: The Scientific Basis*. Cambridge Univ Press, Cambridge, UK.

Stahl, K. (2001) Hydrological drought - a study across Europe. Albert-Ludwigs Universität Freiburg, Freiburg.

Stahl, K. and Demuth, S. (1999) Linking streamflow drought to the occurrence of atmospheric circulation patterns. *Hydrological Sciences Journal-Journal Des Sciences Hydrologiques* **44**, 467-482.

Tate, E. and Gustard, A. (2000) Drought definition: a hydrological perspective. In: *Drought and Drought Mitigation in Europe*, (ed. by J. V. Vogt and F. Somma), 23-48. Kluwer.

Zaidman, M. D., Rees, G. and Gustard, A. (2001) Drought visualization. In: *Assessment of the Regional Impact of Droughts in Europe* (ed. by S. Demuth and K. Stahl), 111-124.

la température de
de

$$Q_s = h \cdot A_b \cdot [\theta$$

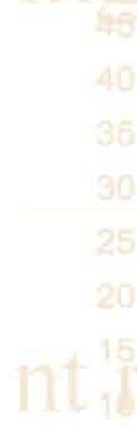
duit $[\beta \cdot s$

B

$$DM = \int \varepsilon_s$$

kg / s

inge kg / s



nt remplacé pa



Direction générale
Parc de Tourvoile
BP 44, 92163 Antony cedex
Tél. 01 40 96 61 21 – Fax 01 40 96 62 95
Web : <http://www.cemagref.fr>